The termination of UHRF1-dependent PAF15 ubiquitin signaling is regulated by USP7 and ATAD5

Ryota Miyashita[1], Atsuya Nishiyama[1], Yoshie Chiba[1], Satomi Kori[3], Norie Kato[3], Chieko Konishi[1], Soichiro Kumamoto[1], Hiroko Kozuka-Hata[2], Masaaki Oyama[2], Yoshitaka Kawasoe[4], Toshiki Tsurimoto[4], Tatsuro S Takahashi[4], Kyohei Arita[3], Makoto Nakanishi[1]

[1]Division of Cancer Cell Biology, The Institute of Medical Science, The University of Tokyo, 4-6-1 Shirokanedai, Tokyo, Japan

[2]Medical Proteomics Laboratory, The Institute of Medical Science, The University of Tokyo, 4-6-1 Shirokanedai, Tokyo, Japan

[3]Structural Biology Laboratory, Graduate School of Medical Life Science, Yokohama City University, 1-7-29, Suehiro-cho, Kanagawa, Japan

[4]Laboratory of Chromosome Biology, Department of Biology, Faculty of Science, Kyushu University, 744, Motooka, Nishi-ku, Fukuoka, Japan

Corresponding author

* To whom correspondence should be addressed. Tel: 81-3-5449-5341; Fax: 81-3-5449-5342; Email: mkt-naka@g.ecc.u-tokyo.ac.jp

Correspondence may also be addressed to Atsuya Nishiyama. Tel: 81-3-5449-

5731; Fax: 81-3-5449-5342; Email: uanishiyama@g.ecc.u-tokyo.ac.jp

Abstract

UHRF1-dependent ubiquitin signaling plays an integral role in the regulation of maintenance DNA methylation. UHRF1 catalyzes transient dual mono-ubiquitylation of PAF15 (PAF15Ub2), which regulates the localization and activation of DNMT1 at DNA methylation sites during DNA replication. Although the initiation of UHRF1-mediated PAF15 ubiquitin signaling has been relatively well characterized, mechanisms underlying its termination and how they are coordinated with the completion of maintenance DNA methylation have not yet been clarified. This study shows that deubiquitylation by USP7 and unloading by ATAD5 (ELG1 in yeast) are pivotal processes for the removal of PAF15 from chromatin. On replicating chromatin, USP7 specifically interacts with PAF15Ub2 in a complex with DNMT1. USP7 depletion or inhibition of the interaction between USP7 and PAF15 results in abnormal accumulation of PAF15Ub2 on chromatin. Furthermore, we also find that the non-ubiquitylated form of PAF15 (PAF15Ub0) is removed from chromatin in an ATAD5-dependent manner. PAF15Ub2 was retained at high levels on chromatin when the catalytic activity of DNMT1 was inhibited, suggesting that the completion of maintenance DNA methylation is essential for termination of UHRF1-mediated ubiquitin signaling. This finding provides a molecular understanding

of how the maintenance DNA methylation machinery is disassembled at the end of the S phase. (200 words)

Introduction

DNA methylation at CpG dinucleotide is an epigenetic modification that regulates various biological processes, including gene silencing, genome stability, cellular development, and differentiation (Greenberg & Bourc'his, 2019; Jones, 2012; Moore et al., 2013). DNA methylation is stably maintained during cell proliferation (Jones & Liang, 2009; Petryk et al., 2021). DNA methyltransferase 1 (DNMT1) plays a key role in the maintenance of DNA methylation by catalyzing the conversion of hemi-methylated DNA to a fully methylated state (Edwards et al., 2017). In addition, recent studies have also suggested the potential de novo function of DNMT1 (Haggerty et al., 2021; Li, Jialun et al., 2020; Li, Yingfeng et al., 2018). Besides the C-terminal catalytic domain, DNMT1 contains several regulatory regions, including Proliferating cell nuclear antigen (PCNA)-interacting protein motif (PIP-box), replication foci targeting sequence (RFTS), a CXXC zinc finger domain, and two bromo-adjacent homology (BAH) domains (Lyko, 2018). DNMT1 specifically localizes at DNA methylation sites dependently on the RFTS domain, which interacts with dual mono-ubiquitylated histone H3 (H3Ub2) or PAF15 (PAF15Ub2) (Ishiyama et al., 2017; Nishiyama et al., 2020; Qin et al., 2015). The RFTS domain of DNMT1 also shows preferential H3K9me3 binding over H3K9me0 to

63 enhance the interaction with H3Ub2 (Ren et al, 2020). These interactions also
64 cause release of autoinhibition and enzymatic activation of DNMT1,
65 presumably via the conformational change (Ishiyama et al., 2017; Mishima et al.,
66 2020; Syeda et al., 2011; Takeshita et al., 2011; Zhang, Liu, et al., 2015).

67 Dual monoubiquitylation of histone H3 and PAF15 is catalyzed by an
68 E3 ubiquitin ligase Ubiquitin-like containing PHD and RING finger domains 1
69 (UHRF1), also known as NP95 or ICBP90 (Karg et al., 2017; Nishiyama et al.,
70 2013). UHRF1 binds specifically to hemi-methylated DNA via its SET and
71 RING-associated (SRA) domain (Arita et al., 2008; Avvakumov et al., 2008;
72 Hashimoto et al., 2008) and plays an essential role for the DNMT1 recruitment
73 to sites of DNA methylation (Bostick et al., 2007; Sharif et al., 2007). The E3
74 ubiquitin ligase activity of UHRF1 is enhanced by binding to hemi-methylated
75 DNA (Harrison et al., 2016), and mutations in the RING finger domain, which is
76 responsible for ubiquitin ligase activity, impair the localization of DNMT1 to
77 methylation sites and maintenance DNA methylation (Nishiyama et al., 2013;
78 Qin et al., 2015). The N-terminal Ubiquitin-like (UBL) domain promotes
79 interaction with the E2 enzyme, Ubch5/UBE2D (DaRosa et al., 2018; Foster et al.,
80 2018). The plant homeodomain (PHD) and tandem Tudor (TTD) domains are
81 responsible for recognizing and binding to the N-terminal portion of histone H3
82 and PAF15 (Arita et al., 2012; Nishiyama et al., 2020; Rajakumara et al., 2011;

Rothbart et al., 2012). UHRF1 dissociates from chromatin upon conversion of hemi-methylated DNA to fully methylated DNA, leading to the inactivation of UHRF1-dependent ubiquitin signaling (Nishiyama et al., 2020).

PAF15 is a PCNA-binding protein (De Biasio et al., 2015; Emanuele et al., 2011; Karg et al., 2017; Nishiyama et al., 2020; Yu et al., 2001) and transiently binds to chromatin during S phase in PCNA- and DNA replication-dependent manner (Nishiyama et al., 2020). In addition, inhibition of UHRF1-dependent PAF15 ubiquitylation significantly impairs PAF15 chromatin binding (Karg et al., 2017; Nishiyama et al., 2020), suggesting that ubiquitylation of PAF15 plays an important role not only in its interaction with DNMT1 but also in its own chromatin binding. Given that more than 80% of CpG methylation on the genome is maintained by DNA replication-coupled maintenance (Charlton et al., 2018; Ming et al., 2020) and that PAF15Ub2 is a key regulator of replication-coupled DNMT1 chromatin recruitment, a regulatory mechanism for PAF15 ubiquitylation is critical for faithful propagation of DNA methylation patterns. Inefficient termination of PAF15 ubiquitin signaling will result in overloading of DNMT1 and unregulated DNA methylation, which is frequently observed in various types of tumors. However, it is not fully understood how the termination of PAF15 ubiquitin signaling is regulated during the process of maintenance DNA methylation.

Protein ubiquitylation is a reversible post-translational modification (Komander & Rape, 2012). Among nearly 100 deubiquitylating enzymes, USP7 (Ubiquitin-Specific Protease 7, also known as HAUSP) has been shown to accumulate at DNA methylation sites in a complex with DNMT1 or UHRF1 (Felle et al., 2011; Ma et al., 2012; Qin et al., 2011; Yamaguchi et al., 2017; Zhang, Rothbart, et al., 2015). While it has been reported that USP7 promotes efficient maintenance of DNA methylation through stabilization of DNMT1 and UHRF1 by preventing their polyubiquitylation and proteasomal degradation (Cheng, Yang, et al., 2015; Du et al., 2010), recent studies have shown that USP7 also modulates the level of ubiquitinated histone H3 and histone H2B on chromatin (Li et al., 2020; Yamaguchi et al., 2017). However, it remains unclear whether USP7 also regulates the PAF15 ubiquitylation.

In this report, we set out to study the molecular mechanism of PAF15 chromatin unloading to understand how the termination of maintenance DNA methylation is regulated. Using the cell-free system derived from *Xenopus* egg extracts that recapitulate the processes of maintenance DNA methylation, we demonstrate that the unloading of PAF15Ub2 is regulated by the two regulatory mechanisms, namely USP7-dependent deubiquitylation and unloading of PAF15 by ATPase family AAA domain-containing protein 5 (ATAD5). We also find that PAF15 unloading is tightly coordinated with the

123 completion of maintenance DNA methylation and requires the release of
124 UHRF1 from chromatin. Finally, co-depletion of USP7 and ATAD5 from egg
125 extracts results in an elevated global DNA methylation. We propose that timely
126 inactivation of PAF15 is critical for the faithful inheritance of DNA methylation
127 patterns.
128
129 **Results**
130 **Identification of USP7 as a PAF15 binding protein**
131 UHRF1-dependent ubiquitin signaling plays a critical role in PAF15
132 chromatin binding. To test whether the deubiquitylation (DUB) activity is
133 required for termination of PAF15 ubiquitylation signaling, we employed
134 Ubiquitin vinyl sulfone (UbVS), a pan DUB inhibitor (Borodovsky et al., 2001).
135 In *Xenopus* egg extracts, sperm chromatin added to egg cytoplasm assembles a
136 functional nucleus and undergoes chromosomal replication (Blow & Laskey,
137 2016). As it has been reported that treatment of *Xenopus* egg extracts with UbVS
138 inhibits ubiquitin turnover, resulting in depletion of free ubiquitin (Dimova et
139 al., 2012), we also added excess free ubiquitin before incubation with sperm
140 chromatin to activate ubiquitylation pathways. As previously reported, PAF15
141 underwent dual mono-ubiquitylation on chromatin during S phase and then
142 dissociated from chromatin (Nishiyama et al., 2020; Povlsen et al., 2012). The

addition of UbVS alone significantly delayed PAF15 and DNMT1 chromatin loading, confirming the importance of ubiquitin signaling for the initiation of maintenance of DNA methylation (Fig. 1A, S1A). In contrast, inhibition of DUB by UbVS plus excess free ubiquitin led to enhanced and prolonged chromatin association of DNMT1 and PAF15, indicating that the DUB activity was required for the termination of maintenance DNA methylation in egg extracts.

To examine the possibility that PAF15 interacts proteins related to deubiquitylation, we performed glutathione-S-transferase (GST)-PAF15 pull-down and nanoflow liquid chromatography-tandem mass spectrometry (nanoLC-MS/MS) for identification of proteins. Sepharose beads bound to GST or GST-PAF15 were incubated with *Xenopus* interphase egg extracts. Beads-bound proteins were eluted by cleavage of GST with thrombin protease (Fig. 1B). Recovered proteins were identified by nanoLC-MS/MS (Fig. 1C, Supplementary Tables 1 and 2). This analysis confirmed the PAF15 binding with PCNA and revealed the interaction between PAF15 and USP7. The interaction between GST-PAF15 and USP7 was also validated by immunoblotting using USP7 specific antibodies. Mutations of two phenylalanine to alanine within the consensus PIP sequence of PAF15 abolished the interaction with PCNA, but not USP7, suggesting that the PAF15-USP7 interaction is independent of PCNA (Fig. 1D, S1B). This interaction was further

163 demonstrated by reciprocal immunoprecipitation and western blotting
164 experiments for endogenous proteins in egg extracts using anti-PAF15 and
165 USP7 antibodies (Fig. 1E). Our results indicate that USP7 has an activity to
166 interact with PAF15 although it was still unclear at this stage whether other
167 protein(s) might be involved in this interaction.

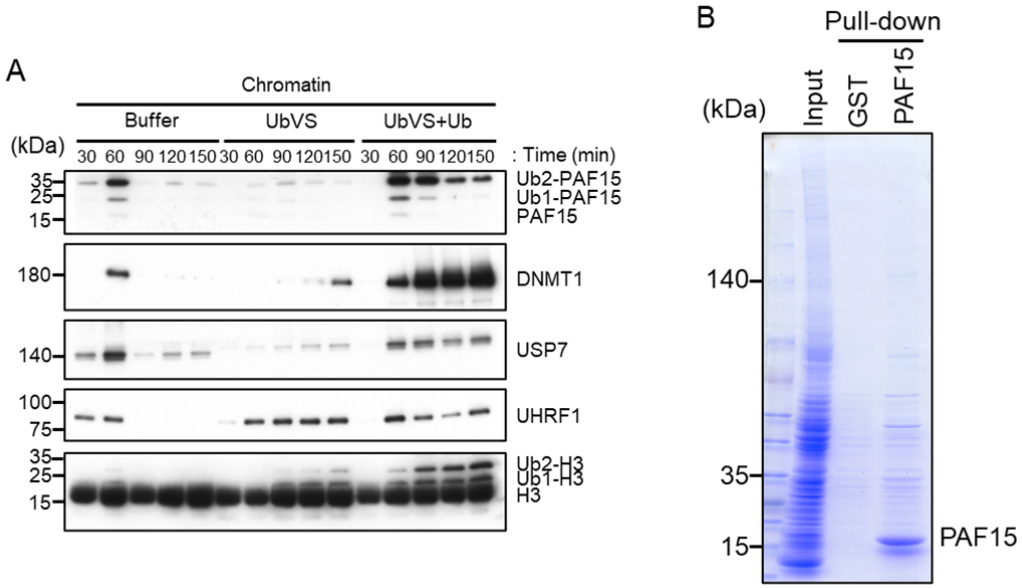

C

Protein Name	Number of detected peptides	
	GST	GST-xPAF15
USP7	0	46
PCNA	1	18

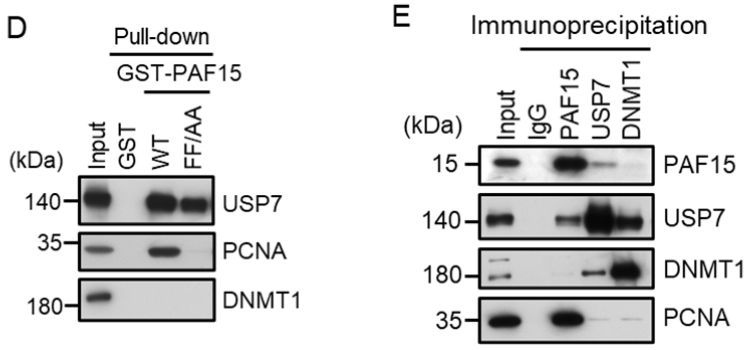

Figure 1. USP7 was identified as a PAF15 binding protein.

(A) Sperm chromatin was added to interphase egg extracts supplemented with either buffer (+Buffer), 20 μM UbVS (+UbVS), or 20 μM UbVS and 58 μM ubiquitin (+UbVS+Ub). Samples were analyzed by immunoblotting using the

antibodies indicated. (B) Proteins pull-downed from interphase egg extracts by GST and GST-PAF15 were stained by CBB. (C) The samples from GST-PAF15 pulldown were analyzed by nanoLC-MS/MS. Selected proteins were indicated in the table. (D) GST pull-down assay was performed by GST or GST-PAF15 wild-type (WT) or PIP mutant (FF/AA), and the samples were analyzed by immunoblotting using the antibodies indicated. (E) Immunoprecipitation was performed by PAF15, USP7 and DNMT1 antibodies-bound beads, and the samples were analyzed by immunoblotting using the antibodies indicated. Source Data are provided as Figure 1-source data.

PAF15 associates with USP7 through the TRAF and UBL2 domains

It has been reported that the binding of USP7 to substrate proteins involves two distinct domains: one is the N-terminal TRAF (TNF-receptor-associated factors-like) domain and the other is the C-terminal UBL (Ubiquitin-like) domain (Al-Eidan et al., 2020). Previous reports have shown that the recognition of the P/A/ExxS motif via the binding pocket within the TRAF domain of USP7 is important for the interaction with many substrate proteins such as p53, MDM2, and MCM-BP (Hu et al., 2006; Jagannathan et al., 2014; Sheng et al., 2006). Meanwhile, it has also been reported that the UBL2 domain recognizes KxxxK motifs that interact with acidic surface patches within the

193 UBL2 (Cheng, Li, et al., 2015). We searched for these motifs in PAF15 and found
194 two P/AxxS motifs (^{76}PSTS^{79}, ^{94}AGGS^{97}) and one KxxxK motif (^{101}KKPRK^{105}) (Fig.
195 2A). We then tested whether these sequences serve as binding sites for USP7 by
196 mutating serine residues in the P/AxxS motif and two lysine residues in the
197 KxxxK motif to alanine (rPAF15 SA and KA, respectively), and combining these
198 mutations to produce a triple mutant (rPAF15 SAKA). As described above,
199 GST-PAF15 was able to pull down both USP7 and PCNA from *Xenopus*
200 interphase egg extracts (Fig. 2B). The PIP-box mutant of PAF15 lost interaction
201 with PCNA but retained binding to USP7. In contrast, mutations in the P/AxxS
202 or KxxxK motifs reduced the binding of USP7 to GST-PAF15. Furthermore, the
203 triple mutations completely lost the binding of PAF15 to USP7. These results
204 suggest that USP7 interacts with PAF15 through both the TRAF domain and the
205 UBL2 domain.

206 Next, we confirmed the requirement of the TRAF and UBL2 domains
207 of USP7 for the interaction with PAF15 by performing pull-down experiments
208 from egg extracts using 3xFLAG-tagged-rUSP7 and its mutants expressed in
209 insect cells (Fig. 2C). The TRAF domain (residues 1-208) interacted efficiently
210 with PAF15, while the catalytic domain (residues 209-582) and UBL1-5 domain
211 (residues 583-1192) of USP7 did not (Fig. 2D). Deletion of the TRAF domain
212 significantly impaired the interaction between PAF15 and USP7, although it did

not affect the binding to DNMT1. This is further supported by the observation that the introduction of the W167A mutation, which disrupts the TRAF binding pocket (Sheng et al., 2006), resulted in a loss of interaction with PAF15. Deletion of the UBL domain or mutations into the UBL2 pocket, D758A/E759A/D764A (Cheng, Yang, et al., 2015), also decreased binding to PAF15. Since the UBL1-5 domain alone is not sufficient for PAF15 binding, this interaction might only occur in the context of the full-length protein. Taken together, these results indicate that both the TRAF and UBL2 domains of USP7 contribute to the interaction with PAF15, as has been recently reported for other USP7 substrates (Ashton et al., 2021; Georges et al., 2019).

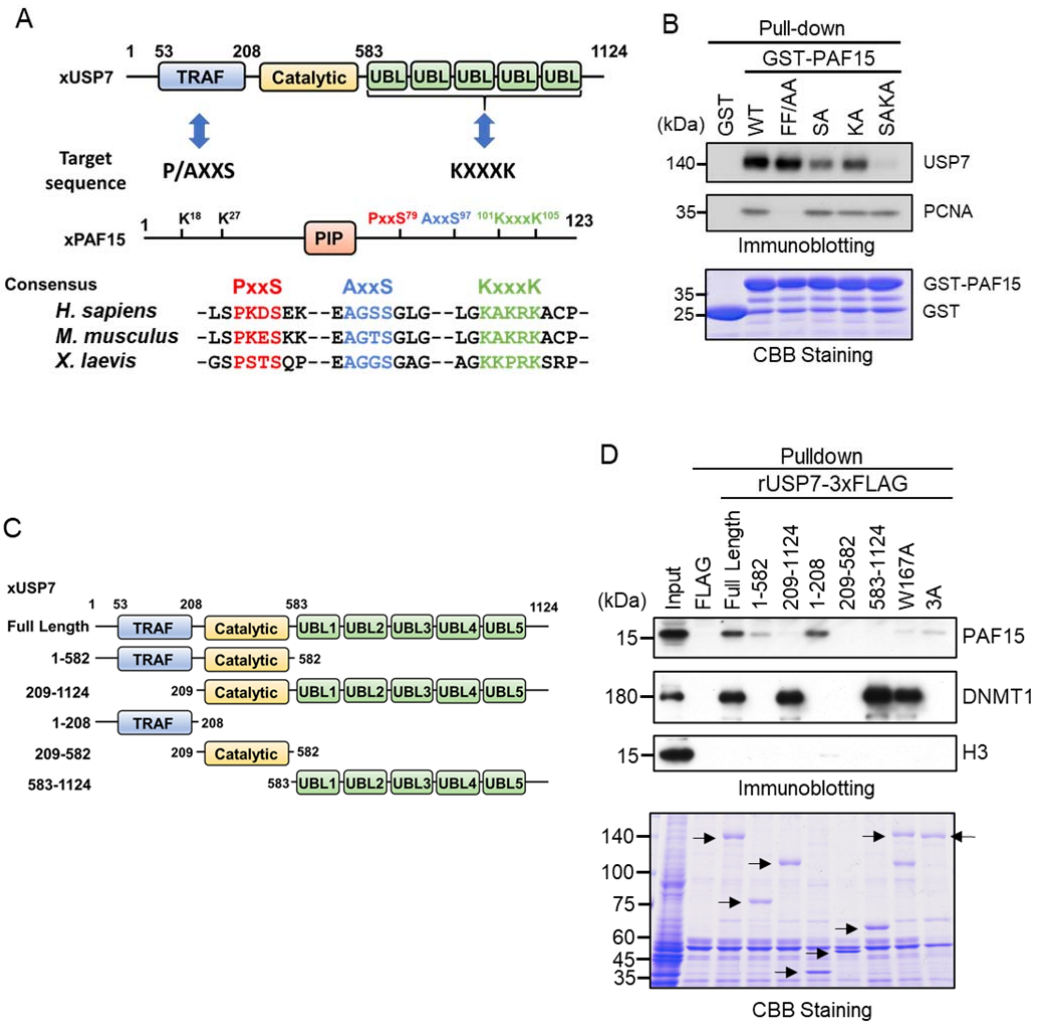

Figure 2. PAF15 associates with the TRAF and UBL1-2 domains of USP7.

(A) Schematic illustration of PAF15-USP7 binding experiment. USP7 recognizes P/AxxS or KxxxK motifs in its substrates via TRAF or UBL domains, respectively. PAF15 has three motifs, and alanine mutations were introduced at S79, S97, K101 and K105. **(B)** GST pull-down from the interphase egg extracts using GST-PAF15, P/AxxS mutant (S79A/S97A; SA), KxxxK mutant (K101A/K105A; KA), and triple mutant (SAKA). The samples were analyzed by

231 immunoblotting using the antibodies indicated. Purified GST or GST-PAF15
232 mutants used in pull-down assay were stained using CBB. **(C)** Schematic
233 illustration of rUSP7 truncation mutants employed in (D). **(D)** FLAG pull-down
234 from interphase egg extracts using rUSP7-3xFLAG mutants presented in (C),
235 W167A and 3A point mutants. USP7 3A: D780A/E781A/D786A. The samples
236 were analyzed by immunoblotting using the antibodies indicated. Samples
237 were also stained by CBB. Arrowheads indicate rUSP7 truncation mutants and
238 point mutants. Source Data are provided as Figure 2-source data.
239
240 **USP7 is involved in PAF15 dissociation from chromatin during S phase**
241 **progression**
242 We next tested whether USP7 regulates PAF15 on chromatin. To this
243 end, we examined the chromatin binding of a recombinant PAF15 mutant
244 lacking USP7 binding activity in PAF15-depleted extracts. As seen for
245 endogenous PAF15, wild-type rPAF15 dissociated from chromatin at 120 min
246 when added to PAF15-depleted egg extracts (Fig. 3A, S2A). In contrast, the
247 rPAF15 with mutated USP7 interacting sequences (SAKA) showed prolonged
248 chromatin association even after 120 min, although chromatin binding of USP7
249 was not affected. To directly test the importance of USP7 for regulation of
250 PAF15 chromatin binding, we depleted USP7 from egg extracts. Compared to

the control, the USP7-depleted extracts showed impaired dissociation of PAF15 chromatin (Fig. 3B, S2B). Affinity-purified recombinant USP7 efficiently restored PAF15 chromatin dissociation, but the USP7 C225S, C223 in human, catalytic inactive mutant failed to do so (Hu et al., 2002; Li et al., 2002) (Fig. 3B, S2B). The USP7 specific inhibitor FT671 also suppressed the PAF15Ub2 chromatin dissociation (Fig. 3C, S2C). These results suggested that USP7 regulates PAF15 chromatin dissociation through its deubiquitylation activity. To investigate whether USP7 directly deubiquitylates PAF15, we performed an *in vitro* deubiquitylation assay by using purified recombinant ubiquitylated hPAF15 and hUSP7. We ubiquitylated hPAF15 by incubating with E1 (mouseUBA1), E2 (UBE2D3), E3 (UHRF1) enzymes *in vitro*. After purification, we incubated ubiquitylated hPAF15 with recombinant hUSP7 and analyzed the reaction products. USP7 WT efficiently deubiquitylated PAF15 while the catalytic inactive USP7 mutant (C223A) did not (Fig. 3D). USP47 that is closely related DUB to USP7 did not show deubiquitylation activity toward the ubiquitylated PAF15 (Fig. S2D). These results suggested that USP7 directly deubiquitylates PAF15 to promote PAF15 chromatin dissociation.

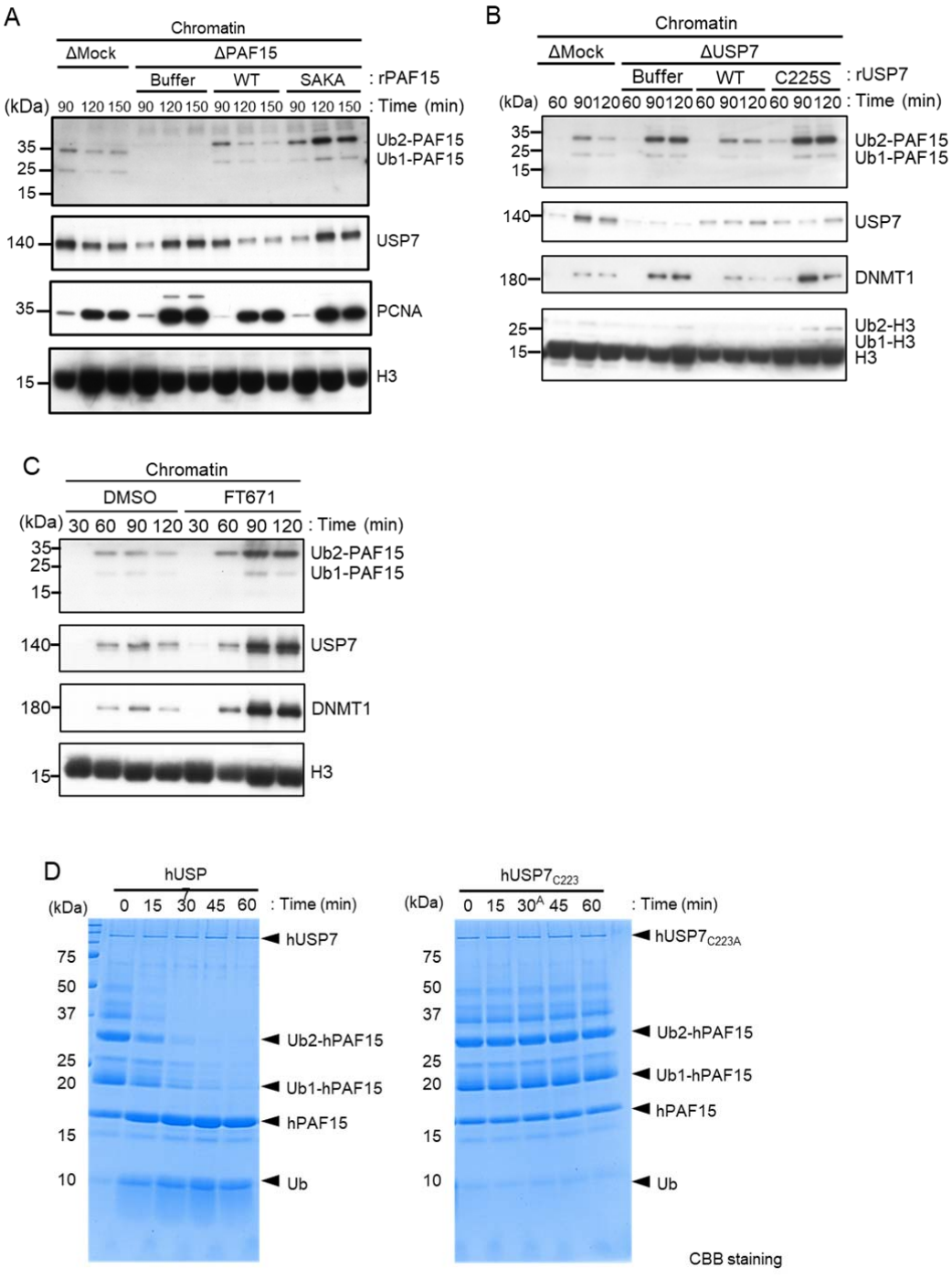

Figure 3. USP7 promotes PAF15 dissociation from chromatin.

(A) Sperm chromatin was added to Mock- or PAF15-depleted interphase extracts supplemented with either buffer (+Buffer), wild-type rPAF15-3xFLAG (+WT) or rPAF15 SAKA-3xFLAG (+SAKA). Chromatin fractions were isolated, and the samples were analyzed by immunoblotting using the antibodies indicated. **(B)** Sperm chromatin was added to Mock- or USP7-depleted interphase extracts supplemented with either buffer (+Buffer), wild-type rUSP7-3xFLAG (+WT) or catalytic mutant rUSP7 C225S-3xFLAG (+C225S). Chromatin fractions were isolated, and the samples were analyzed by immunoblotting using the antibodies indicated. (C) Sperm chromatin was added to interphase extracts supplemented with either DMSO (+DMSO), or FT671 (+FT671). Chromatin fractions were isolated, and the samples were analyzed by immunoblotting using the antibodies indicated. (D) Ubiquitylated hPAF15 was incubated with recombinant hUSP7 WT (left) or C223A catalytic mutant (right) at indicated times. The reaction products were analyzed by SDS-PAGE with CBB staining. Source Data are provided as Figure 3-source data.

To further elucidate the mechanism underlying termination of PAF15 signaling by USP7, we examined whether USP7 interacts with PAF15 on chromatin. As shown in previous reports (Nishiyama et al., 2020), chromatin-

292 bound PAF15 existed mainly as ubiquitylated forms (PAF15Ub2 or PAF15Ub1),
293 and PAF15Ub2 specifically interacted with DNMT1 (Fig. 4A). USP7 co-
294 immunoprecipitated with PAF15 as well as DNMT1. Importantly, PAF15Ub2
295 was readily detected in the USP7 immunoprecipitates, whereas PAF15Ub1 and
296 PAF15Ub0 were not. Given that DNMT1 forms a complex with USP7 and
297 predominantly binds to PAF15Ub2, USP7 binding to PAF15 might be mediated
298 by DNMT1 at DNA methylation sites.

299 In order to inhibit the interaction between DNMT1 and USP7, we
300 introduced mutations into the KG linker of DNMT1, which is responsible for
301 USP7 binding (Cheng, yang, et al., 2015; Yamaguchi et al., 2017). We performed
302 immunodepletion of endogenous DNMT1 from egg extracts and added-back
303 wild-type DNMT1 or the KG linker mutant (DNMT1 4KA). As previously
304 reported, immunodepletion of DNMT1 inhibited the chromatin binding of
305 USP7 and induced marked accumulation of ubiquitylated PAF15 and histone
306 H3 (Nishiyama et al., 2013; Nishiyama et al., 2020). Wild-type DNMT1
307 efficiently restored USP7 chromatin recruitment and PAF15 chromatin
308 dissociation, but DNMT1 4KA failed to do so (Fig. 4B, C, S3A). These results
309 suggest that DNMT1 recruits USP7 to chromatin and mediates the formation of
310 USP7-PAF15Ub2 complex. Consistent with this idea, immunodepletion of
311 PAF15 had no significant effect on the level of chromatin-bound USP7 (Fig. 4D,

S3B).

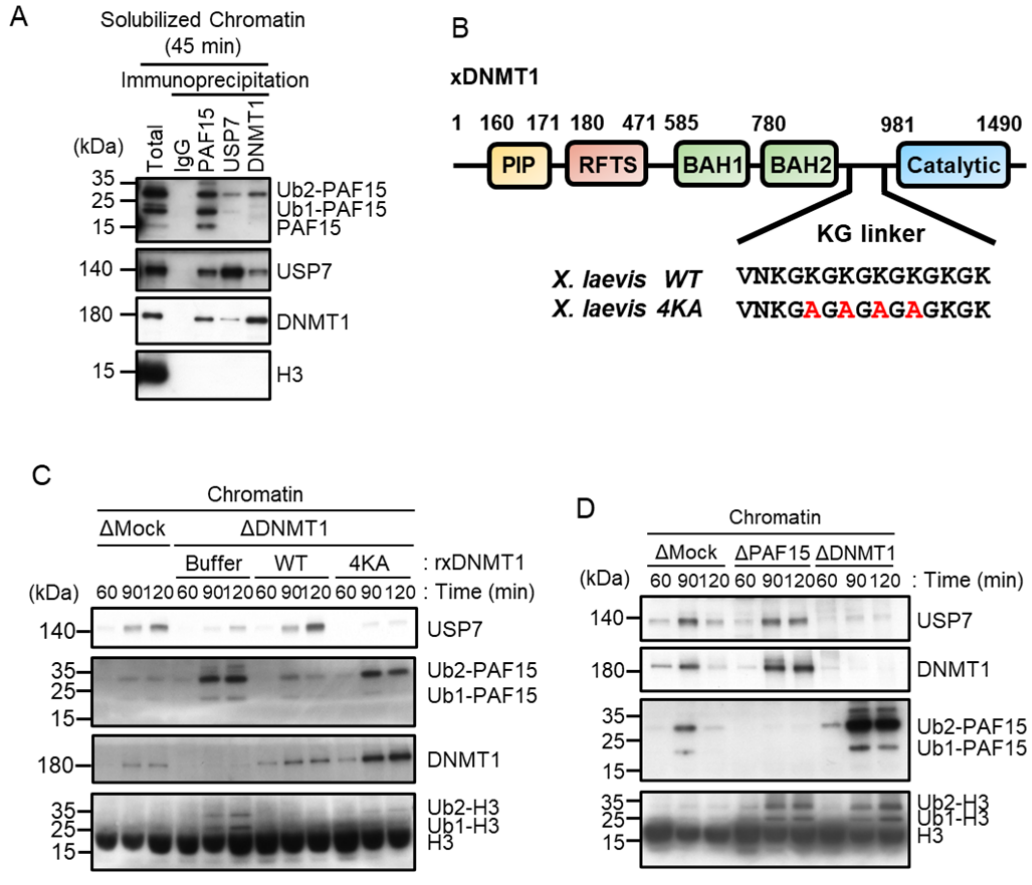

Figure 4. USP7 is recruited to chromatin through the interaction with DNMT1 for PAF15 deubiquitylation.

(A) Sperm chromatin was added to interphase extracts. Replicating chromatin was digested by micrococcal nuclease (MNase). Immunoprecipitation was performed by PAF15, USP7 and DNMT1 antibodies from the solubilized chromatin fraction, and the samples were analyzed by immunoblotting using the antibodies indicated. **(B)** Illustration of DNMT1 domain structure. The KG linker located between the BAH domain and catalytic domain contributes to

interaction with USP7. rDNMT1 4KA mutant, using in (C), was introduced mutation at four lysines to alanine in the KG linker. **(C)** Sperm chromatin was added to Mock- or DNMT1-depleted interphase extracts supplemented with either buffer (+Buffer), wild-type rDNMT1-3xFLAG (+WT), or rDNMT1 4KA-3xFLAG (+4KA). Chromatin fractions were isolated, and the samples were analyzed by immunoblotting using the antibodies indicated. **(D)** Sperm chromatin was added to Mock-, PAF15-, and DNMT1-depleted extracts. Chromatin fractions were isolated, and the samples were analyzed by immunoblotting using the antibodies indicated. Source Data are provided as Figure 4-source data.

Unloading of PAF15 couples with the completion of DNA methylation maintenance

We next tested how PAF15 chromatin dissociation is coordinated with the progression of maintenance DNA methylation. Completion of DNA maintenance methylation is accompanied by conversion of hemimethylated DNA to fully methylated DNA by DNMT1 and subsequent inactivation of UHRF1-dependent ubiquitin signaling. To inhibit DNMT1 activity, we replaced the endogenous DNMT1 with a recombinant DNMT1 C1101S mutant that lacks DNMT1 catalytic activity (Takebayashi et al., 2007; Takeshita et al.,

2011; Wyszynski et al., 1993). The results showed that the inactivation of DNMT1 led to accumulation of UHRF1 on chromatin, presumably due to the failure in the conversion of hemi-methylated DNA to fully methylated state (Fig. 5A, S4A). PAF15Ub2 showed a significant accumulation on chromatin along with H3Ub2 under this condition, suggesting that the completion of maintenance DNA methylation is required for the USP7-dependent dissociation of PAF15 from chromatin. Note that the recruitment of USP7 to chromatin was rather enhanced when DNMT1 was inactivated (Fig. 5A). Immunoprecipitation of PAF15 or USP7 from chromatin lysates showed that inhibition of the catalytic activity of DNMT1 did not affect the binding of USP7 to PAF15Ub2 (Fig. 5B). These results suggest that the USP7-mediated deubiquitylation couples the completion of DNA methylation by DNMT1.

Failure of DNA methylation replication has been shown to be accompanied by accumulation of UHRF1 on chromatin and enhanced UHRF1-dependent ubiquitin signaling. We hypothesized that when maintenance DNA methylation is inhibited, the enhanced E3 ligase activity of UHRF1 caused by its chromatin accumulation may overcome the deubiquitylation activity of USP7, which apparently suppresses the deubiquitylation of PAF15. Recent studies have reported that the maternal gene Stella/DPPA3, which protects against oocyte-specific DNA methylation in mice, binds directly to the UHRF1-PHD

362 domain and inhibits UHRF1 nuclear localization and chromatin binding (Du et
363 al., 2019; Li et al., 2018; Mulholland et al., 2020). We have previously shown that
364 the addition of recombinant mouse DPPA3 to egg extracts inhibits the
365 chromatin-binding activity of UHRF1 and induces dissociation of UHRF1. To
366 determine whether UHRF1 competes with the deubiquitylation by USP7, we
367 forced chromatin dissociation of UHRF1 by adding the purified recombinant
368 GST-mDPPA3 to DNMT1 depleted extracts supplemented with the DNMT1
369 C1101S mutant (Fig. 5C). The addition of recombinant mDPPA3 efficiently
370 induced chromatin dissociation of UHRF1, leading to a significant decrease in
371 the levels of chromatin-bound PAF15 and DNMT1 (Fig. 5D, S4B). Importantly,
372 USP7 depletion caused significant delay of PAF15 chromatin dissociation
373 induced by mDPPA3 addition. These results suggest that UHRF1 maintains
374 PAF15 chromatin association by counteracting USP7-dependent PAF15
375 deubiquitylation until the completion of maintenance DNA methylation.

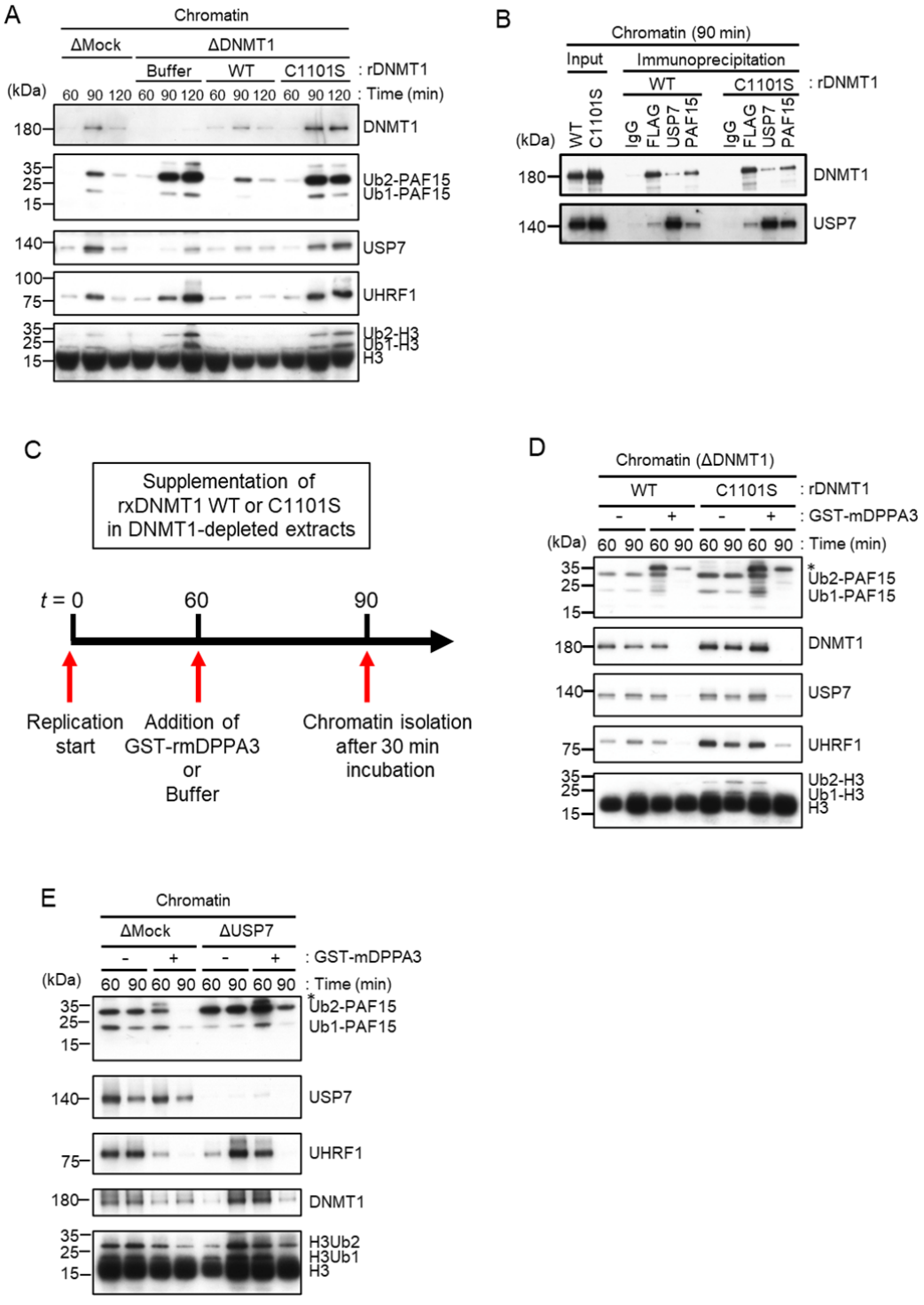

Figure 5. Unloading of PAF15 requires DNMT1-dependent DNA methylation.

(A) Sperm chromatin was added to Mock- or DNMT1-depleted interphase extracts supplemented with either buffer (+Buffer), wild-type rDNMT1-3xFLAG (+WT), or catalytic mutant rDNMT1 C1101S-3xFLAG (+C1101S). Chromatin fractions were isolated, and the samples were analyzed by immunoblotting using the antibodies indicated. **(B)** Sperm chromatin was added to DNMT1-depleted interphase extracts supplemented wild-type rDNMT1-3xFLAG (+WT) or catalytic mutant rDNMT1 C1101S-3xFLAG (+C1101S). Replicating chromatin was digested by MNase. Immunoprecipitation was performed by PAF15, USP7 antibodies-bound beads, and FLAG affinity beads in the solubilized chromatin fraction solution, and the samples were analyzed by immunoblotting using the antibodies indicated. **(C)** A schema of an experiment described in Figure 5C. **(D)** Sperm chromatin was added to DNMT1-depleted interphase extracts supplemented wild-type rDNMT1-3xFLAG (+WT) or catalytic mutant rDNMT1 C1101S-3xFLAG (+C1101S). After 60 min, the extracts were supplemented with either buffer (-) or GST-mDPPA3 61-150 (+). Chromatin fractions were isolated, and the samples were analyzed by immunoblotting using the antibodies indicated. The asterisk indicates a non-specific band. **(E)** Sperm chromatin was added to USP7-depleted interphase extracts. After 90 min, the extracts were supplemented with either buffer (-) or GST-mDPPA3 61-150 (+). Chromatin fractions were isolated, and the samples were analyzed by immunoblotting

using the antibodies indicated. The asterisk indicates a non-specific band. Source Data are provided as Figure 5-source data.

ATAD5 promotes PAF15 unloading from chromatin

It has been shown that PCNA is unloaded from chromatin by the ATAD5-RLC (RFC-like complex) in a coordinated manner with the maturation of Okazaki fragment in the late S phase (Johnson et al., 2016; Kang et al., 2019; Kubota et al., 2015; Kubota et al., 2013; Lee et al., 2013; Ulrich, 2013). Based on the requirement of PCNA for PAF15 chromatin loading described previously, we investigated the role of ATAD5 in the chromatin dissociation of PAF15. Consistent with previous reports in mammalian cultured cells and budding yeast, immunodepletion of ATAD5 from interphase egg extracts resulted in the chromatin accumulation of PCNA (Fig. 6A) (Kubota et al., 2013; Lee et al., 2013). Interestingly, chromatin binding of PAF15Ub0 was readily detected on ATAD5-depleted chromatin (Fig. 6A, S5A). On the other hand, no significant change was observed in the amount of PAF15Ub2 on chromatin in ATAD5-depleted extracts. In USP7/ATAD5 co-depleted extracts, PAF15 showed accumulation on chromatin regardless of its ubiquitylation state. The accumulation of the PAF15Ub0 and Ub1 were rescued by recombinant hATAD5-RFCs addition to ATAD5-depleted extracts (Fig. 6B, S5B). These

418 results suggested that ATAD5 regulates PAF15Ub0 and Ub1 chromatin
419 dissociation.

420 We next examined whether ATAD5 regulates chromatin unloading of
421 non-ubiquitylated PAF15. First, we added a PAF15 mutant lacking the
422 ubiquitylation sites (PAF15 KRKR) to the PAF15/ATAD5 double-depleted
423 extract and examined its chromatin binding. As expected, PAF15 KRKR did not
424 show chromatin binding in the presence of ATAD5, but its chromatin binding
425 became detectable in ATAD5-depleted extracts (Fig. 6C, S5C). We also inhibited
426 PAF15 ubiquitylation by UHRF1 depletion. As previously reported, UHRF1
427 depletion completely inhibited PAF15 ubiquitylation and chromatin loading,
428 resulting in inhibition of DNMT1 recruitment (Nishiyama et al., 2020). However,
429 obvious chromatin binding of non-ubiquitylated PAF15 was observed in
430 UHRF1/ATAD5 double-depleted extracts (Fig. 6D, S5D). These results suggest
431 that non-ubiquitylated or deubiquitylated PAF15 is unloaded in an ATAD5-
432 dependent manner.

433

434 **USP7 and ATAD5 promote dissociation of chromatin-bound PAF15**

435 Next, we investigated whether USP7 and ATAD5 accelerates PAF15
436 chromatin dissociation. To induce PAF15 chromatin accumulation, sperm
437 chromatin was incubated in USP7/ATAD5 co-depleted extracts. Chromatin was

438 isolated after 90 min replication and further incubated with recombinant USP7
439 WT or C225S catalytic inactive mutant. PAF15Ub2, but not PAF15Ub1 or
440 PAF15Ub0, was efficiently dissociated from chromatin only when recombinant
441 wild-type USP7 was added (Fig. 6E, S5E). Conversely, when recombinant
442 hATAD5-RLCs was added to USP7/ATAD5 co-depleted extracts after 120 min
443 replication, PAF15Ub1 and Ub0 dissociated from chromatin (Fig. 6F, S5F).
444 These results suggested that chromatin dissociation of PAF15Ub2 is regulated
445 by USP7, whereas PAF15Ub1 and PAF15Ub0 are regulated by ATAD5-
446 dependent unloading.

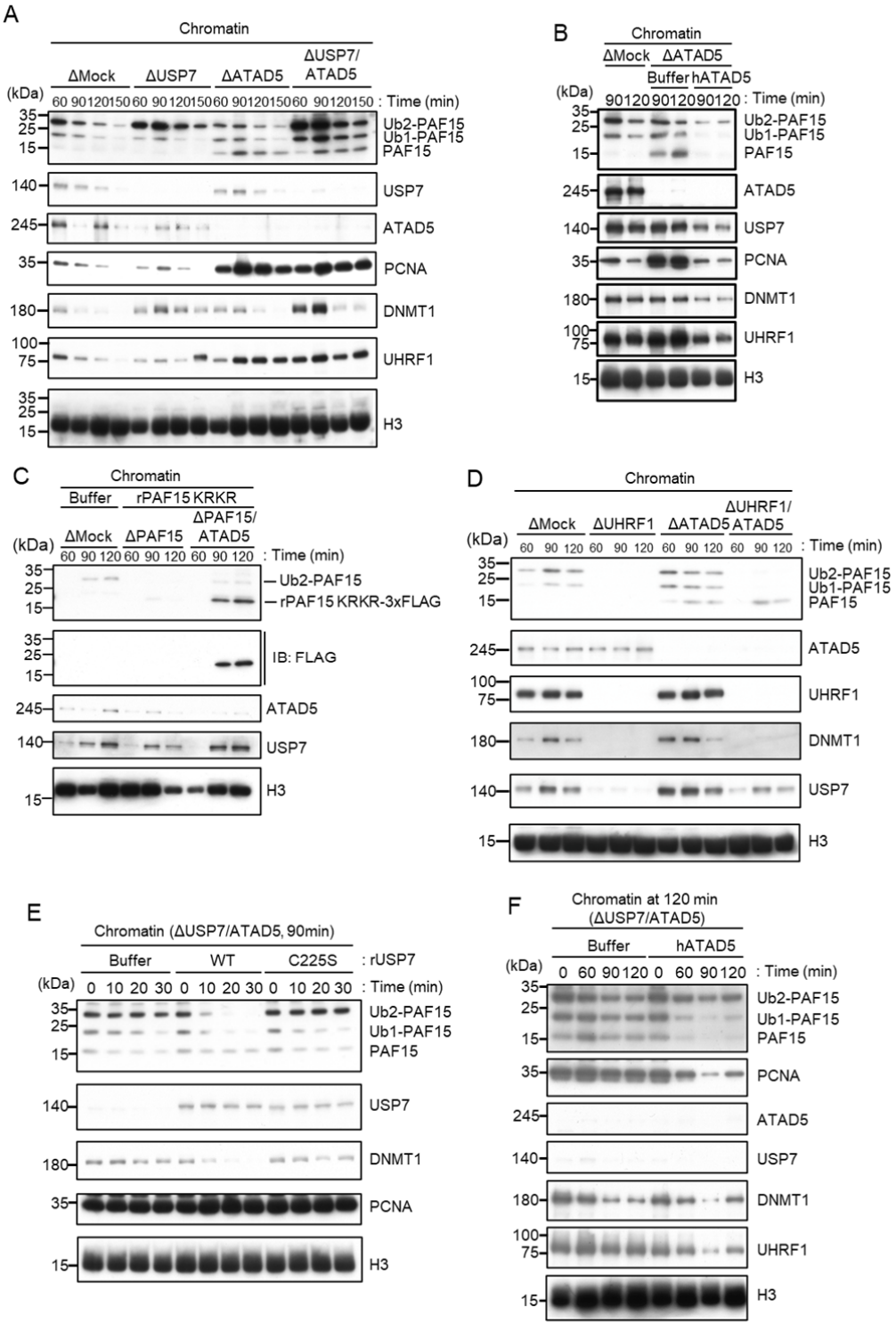

Figure 6. ATAD5 unloads PAF15Ub0 from chromatin.

449 **(A)** Sperm chromatin was added to Mock-, USP7-, ATAD5-, and USP7/ATAD5-
450 depleted interphase extracts, and isolated at indicated time points. Chromatin
451 bound proteins were analyzed by immunoblotting. (B) Sperm chromatin was
452 added to Mock-, ATAD5-depleted interphase extracts supplemented with either
453 buffer (+Buffer) or recombinant hATAD5-RFCs (+ATAD5). Chromatin fractions
454 were isolated, and the samples were analyzed by immunoblotting using the
455 antibodies indicated. **(C)** Recombinant PAF15 K18R/K27R-3xFLAG was
456 supplemented to PAF15-, and PAF15/ATAD5-depleted extracts, and chromatin
457 fractions were isolated. Chromatin bound proteins were confirmed by
458 immunoblotting. **(D)** Sperm chromatin was added to Mock-, UHRF1-, ATAD5-,
459 and UHRF1/ATAD5-depleted extracts, and isolated at indicated time point.
460 Chromatin bound proteins were analyzed by immunoblotting. **(E)** Sperm
461 chromatin was added to USP7/ATAD5-depleted extracts, and isolated at 90 min.
462 The chromatin was supplemented with either buffer (+Buffer), USP7 WT-
463 3xFLAG (+WT), or USP7 C225S-3xFLAG (+C225S) and re-isolated at indicated
464 time points. Chromatin bound proteins were analyzed by immunoblotting. **(F)**
465 Sperm chromatin was added to Mock-, USP7/ATAD5-depleted extracts. After
466 replication at 90 min, the extracts were supplemented with either buffer
467 (+Buffer) or recombinant hATAD5-RFCs (+ATAD5). Chromatin fractions were

468 isolated and the samples were analyzed by immunoblotting using the
469 antibodies indicated. Source Data are provided as Figure 6-source data.
470
471 **Co-depletion of USP7 and ATAD5 leads to an increase in global DNA**
472 **methylation.**
473 Inhibition of chromatin unloading of PAF15 might affect maintenance
474 DNA methylation. To investigate changes in the level of global DNA
475 methylation and efficiency of DNA replication by USP7- and/or ATAD5-
476 depletion, we measured the incorporation of radiolabeled S-adenosyl-
477 methionine (^{3}H-SAM) and [α-^{32}P] dCTP into DNA, respectively. USP7/ATAD5
478 double-depletion caused increased DNA methylation compared to mock-
479 depleted extracts without significant effect on gross DNA replication (Fig. 7,
480 S6A, B), but either USP7- or ATAD5-depletion alone did not do so. These data
481 suggest that the termination of PAF15 ubiquitin signaling suppresses excessive
482 DNA methylation.

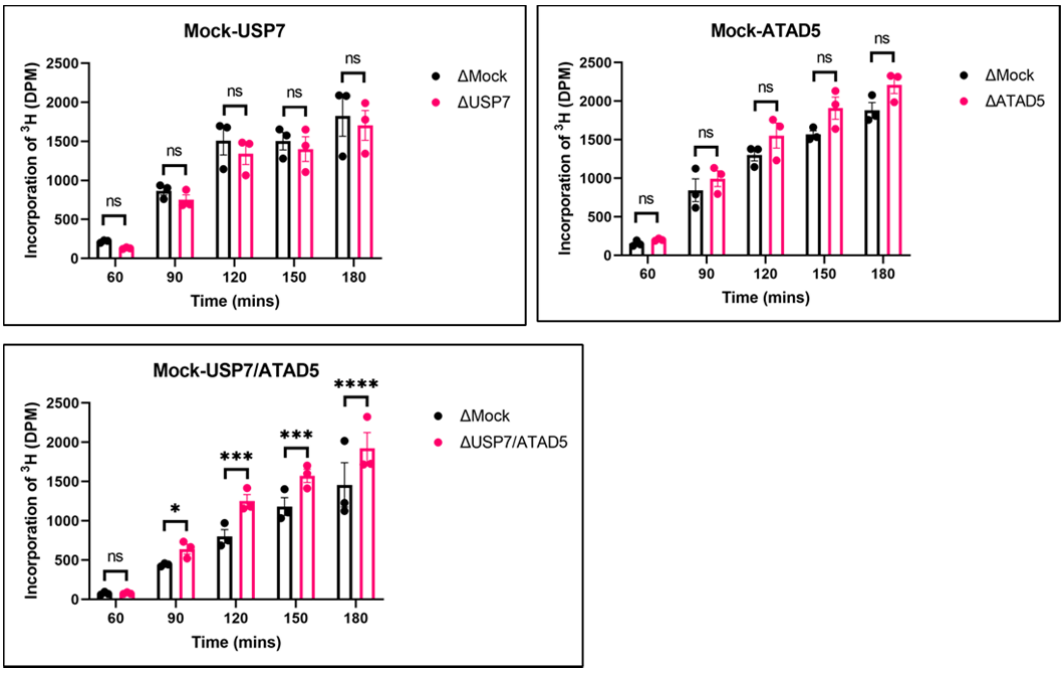

Figure 7. PAF15 dissociation negatively regulates aberrant increase of DNA methylation.

Sperm chromatin and radiolabeled S-[methyl-^{3}H]-adenosyl-L-methionine were added to either Mock- and USP7-, ATAD5-, or USP7/ATAD5 co-depleted extracts. Purified DNA samples were analyzed to determine the efficiency of DNA methylation. Data are presented as mean ± SEM. Multiple comparisons were performed by Two-way Repeated Measure analysis of variance (RM ANOVA) followed by Sidak's multiple comparison test. ns; not significant, *p < 0.05, ***p < 0.001, ****p < 0.0001. Source Data are provided as Figure 7-source data.

Discussion

In this study, we investigated how PAF15 chromatin unloading is regulated during the completion of maintenance DNA methylation. Using *Xenopus* egg extracts, we demonstrate that PAF15 unloading is regulated by two distinct mechanisms. First, USP7 deubiquitylates PAF15Ub2 to promote PAF15Ub2 dissociation from chromatin. Second, the ATAD5-RLCs complex promotes chromatin unloading of non-ubiquitylated PAF15 and PAF15Ub1 together with PCNA. Importantly, our data show that co-depletion of USP7 and ATAD5 leads to chromatin accumulation of DNMT1 together with PAF15Ub2 and increased global DNA methylation. Consistent with this data, previous report also showed that the loss of USP7 in HeLa cells leads to the increase of DNA methylation in a substantial fraction of de novo DNA methylation sites upon long-term culture (Li et al., 2020). We speculate that accumulation of both PAF15Ub2 and PCNA on USP7/ATAD5-depleted chromatin causes premature DNMT1 localization and hyperactivation at de novo DNA methylation sites.

Our data showed that USP7 specifically targets PAF15Ub2 to facilitate its chromatin dissociation; PAF15Ub2 has been reported to interact with the RFTS domain of DNMT1 (Nishiyama et al., 2020), thereby recruiting the DNMT1-USP7 complex to the methylation sites. Since the interaction between USP7 and PAF15 in the cell is probably very weak, the formation of a stable USP7-DNMT1 and PAF15Ub2 complex might be critical for the specific

516 recognition of PAF15Ub2 by USP7. Notably, neither removal nor inhibition of
517 USP7 enhanced histone H3 ubiquitylation, suggesting that PAF15 ubiquitin
518 signaling is the primary pathway to maintain DNA methylation during S phase
519 as previously reported (Nishiyama et al., 2020). Although our results indicate
520 that USP7 functions as the major DUB for PAF15 deubiquitylation, it remains
521 possible that other DUBs also influence this process. Indeed, the gradual
522 decrease in chromatin binding of PAF15Ub2 in the absence of USP7 suggests
523 that other proteins are also involved.

524 Our results also demonstrate that the ATAD5-RLC complex is required
525 for chromatin dissociation of non-ubiquitylated PAF15 and PAF15Ub1. Notably,
526 many of DNA replication proteins interacting with PCNA compete for binding
527 surfaces between ATAD5 and PCNA during DNA replication (Kang et al.,
528 2019). We speculate that PAF15 may not interfere with the interaction between
529 ATAD5 and PCNA due to its small size and flexible structure. Our results
530 suggested that PAF15Ub2 is not targeted by ATAD5-dependent unloading. This
531 is consistent with our previous report that dual mono-ubiquitylation of PAF15
532 plays a pivotal role in its chromatin binding (Nishiyama et al., 2020). However,
533 it is not clear how dual mono-ubiquitylation of PAF15 contributes to stable
534 PAF15 chromatin binding. Interestingly, several studies reported the DNA
535 binding activity of ubiquitin. K63-linked ubiquitin chain binds to DNA directly

through its DNA interacting patch, consists with threonine, lysine, and glutamic acid (Liu et al., 2018). Another paper also has shown that mono-ubiquitylation of transcription factors, such as p53 or IRF1 enhanced their nuclear localization and chromatin binding (Landre et al., 2017). Future biochemical analyses will be required to test whether dual monoubiquitylation enhances DNA binding activity of PAF15. Alternatively, DNMT1, which forms a complex with PAF15Ub2, may prevent ATAD5-dependent unloading by interacting with PCNA via the PIP-box. Intriguingly, the chromatin binding of non-ubiquitylated PAF15 in ATAD5-depleted extracts did not require UHRF1. These data suggest that PCNA-mediated loading of PAF15 could occur at sites outside DNA methylation sites. In such regions, ATAD5 may prevent the formation of the maintenance DNA methylation machinery by excluding the PAF15-PCNA complex from chromatin.

In summary, data presented here suggest that the coupled ubiquitylation and deubiquitylation may be necessary for proper maintenance of DNA methylation. Interestingly, inactivation of DNMT1 catalytic activity almost completely suppressed chromatin dissociation of PAF15. How is the PAF15 inactivation coupled to the completion of methylation for DNA maintenance? Even when DNA methylation was inhibited, chromatin recruitment of USP7 and the formation of the USP7-PAF15Ub2 complex were

observed. Thus, the inhibition of deubiquitylation in this condition is not caused by suppressing USP7 chromatin recruitment or USP7 interaction with PAF15Ub2. Our results suggest that ubiquitylation by UHRF1 is predominant over the deubiquitylation and unloading of PAF15, maintaining PAF15Ub2 until the completion of maintenance methylation by DNMT1. UHRF1 is thought to dissociate from DNA upon binding to hemi-methylated DNA by DNMT1 (Arita et al., 2008). Dissociation of UHRF1 from chromatin upon the conversion of hemi-methylated DNA to fully methylated DNA would trigger the removal of ubiquitin moieties from PAF15 by USP7. It is also possible that the binding of DNMT1 to hemi-methylated DNA induces conformational changes in USP7 or PAF15Ub2 to facilitate the deubiquitylation of PAF15Ub2 by USP7. Detailed analysis of the DNMT1-USP7-PAF15Ub2 complex will be important in future studies.

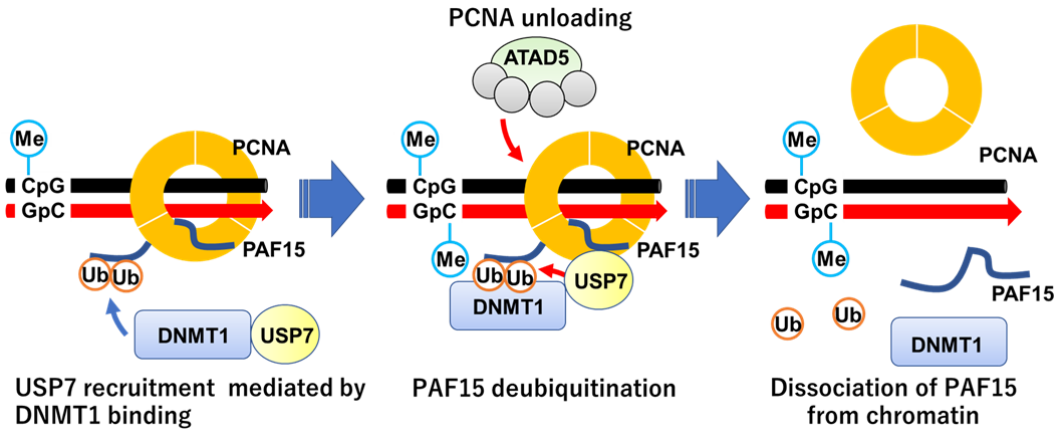

Figure 8. A schematic model of PAF15 deubiquitylation and chromatin unloading

During the S phase, USP7 is recruited to the methylation site along with DNMT1. After the conversion of hemi-methylated DNA to fully methylated DNA by DNMT1, USP7 promotes deubiquitylation of PAF15Ub2. Subsequently, the deubiquitylated PAF15 (PAF15Ub0) is removed from chromatin together with PCNA by the ATAD5-RLC complex.

Methods

Primers

All oligonucleotide sequences are listed in the Supplementary Table 3.

Xenopus egg extracts

Xenopus laevis was purchased from Kato-S Kagaku and handled according to the animal care regulations at the University of Tokyo. The preparation of interphase egg extracts, chromatin isolations, UbVS reactions, DNA replication assays, DNA methylation assays, and immunodepletions were

performed as described previously (Kumamoto et al., 2021; Nishiyama et al., 2020). Unfertilized *Xenopus laevis* eggs were dejellied in 2.5 % thioglycolic acid-NaOH (pH 8.2) and washed in 1xMMR buffer [100 mM NaCl, 2 mM KCl, 1 mM $MgCl_2$, 2 mM $CaCl_2$, 0.1 mM Ethylenediaminetetraacetic acid (EDTA), 5 mM HEPES-NaOH (pH 7.5)]. After activation in 1xMMR supplemented with 0.3 μg/ml calcium ionophore, eggs were washed with EB buffer [50 mM KCl, 2.5 mM $MgCl_2$, 10 mM HEPES-KOH (pH 7.5), 50 mM sucrose]. Eggs were packed into tubes by centrifugation (BECKMAN, Avanti J-E, JS-13.1 swinging rotor) for 1 min at 190 xg and crushed by centrifugation for 20 min at 18,973 xg. Egg extracts were supplemented with 50 μg/mL cycloheximide, 20 μg/mL cytochalasin B, 1 mM dithiothreitol (DTT), 2 μg/mL aprotinin, 5μg/mL leupeptin and clarified by ultracentrifugation (Hitachi, CP100NX, P55ST2 swinging rotor) for 20 min at 48,400 xg. The cytoplasmic extracts were aliquoted, frozen in liquid nitrogen, and stored at -80 °C. All extracts were supplemented with an energy regeneration system (2 mM ATP, 20 mM phosphocreatine, and 5 μg/ml creatine phosphokinase). 3,000-4,000 nuclei/μl of sperm nuclei were added and incubated at 22 °C. Aliquots (15-20 μl) were diluted with 150 μl chromatin purification buffer [CPB; 50 mM KCl, 5 mM $MgCl_2$, 20 mM HEPES-KOH (pH 7.6)] containing 0.1% Nonidet P-40 (NP-40), 2% sucrose, 2 mM N-ethylmaleimide (NEM) and 0.1 mM PR-619. After incubation on ice for 5 min,

608 diluted extracts were layered over 1.5 ml of CPB containing 30% sucrose and
609 centrifuged at 15,000 xg for 10 min at 4 °C. Chromatin pellets were resuspended
610 in 1xLaemmli sample buffer, boiled for 5 min at 100 °C, and analyzed by
611 immunoblotting.

612

613 **Antibodies and immunoprecipitations/immunodepletions**

614 *Xenopus* ATAD5 (xATAD5) antibodies were raised in rabbits by
615 immunization with a His10-tagged recombinant xATAD5 fragment encoding 1-
616 289 amino acids and used for immunodepletion and immunoblotting. Rabbit
617 polyclonal antibodies raised against PAF15, DNMT1, and UHRF1 have been
618 previously described. Rabbit polyclonal USP7 antibody (A300-033A) was
619 purchased from Bethyl Laboratories. Mouse monoclonal antibody against
620 PCNA (PC-10) was purchased from Santa Cruz Biotechnology. Rabbit
621 polyclonal histone H3 antibody (ab1791) was purchased from Abcam. For
622 immunoprecipitation, 10 μl of Protein A agarose (GE Healthcare) was coupled
623 with 2 μg of purified antibodies or 5 μl of antiserum. The agarose beads were
624 washed twice with CPB buffer containing 2% sucrose. The antibody beads were
625 incubated with egg extracts for 2 h at 4 °C. The beads were washed three times
626 with CPB buffer containing 2% sucrose and 0.1% Triton X-100 and resuspended

in 10 μl of 2xLaemmli sample buffer and 20 μl of 1xLaemmli sample buffer. For immunodepletion, 250 μl of antiserum were coupled to 60 μl of recombinant Protein A Sepharose (rPAS, GE Healthcare). Antibodies bound beads were washed three times in CPB and supplemented with 6 μl fresh rPAS. Beads were split into three portions, and 100 μl of extracts were depleted in three rounds at 4 °C, each for 1 h.

GST pull-down assay in *Xenopus* egg extracts

Recombinant GST or GST-PAF15 proteins were expressed and purified from *Escherichia. Coli* (BL21-CodonPlus), and immobilized on Glutathione Sepharose 4B resin (GE Healthcare) for 2 h at 4 °C. The beads were incubated with interphase egg extracts for 2 h at 4 °C. The beads were washed four times with CPB containing 2% sucrose and 0.1% Triton X-100. The washed beads were resuspended in 20 μl of 2xLaemmli sample buffer and 20 μl of 1xLaemmli sample buffer, boiled for 5 min at 100 °C, and analyzed by immunoblotting.

Immunoprecipitation of FLAG-USP7

Recombinant 3xFLAG-tagged USP7 proteins were expressed in Sf9

insect cells. These insect cells were collected and suspended in lysis buffer [20 mM Tris-HCl (pH 8.0), 100 mM KCl, 5 mM $MgCl_2$, 10% glycerol, 1% NP-40, 1 mM DTT, 5 μg/ml leupeptin, 2 μg/ml aprotinin, 20 μg/ml trypsin inhibitor, 100 μg/ml phenylmethylsulfonyl fluoride (PMSF)], followed by incubation on ice for 10 min. Soluble fractions were isolated after centrifugation of the lysate at 15,000 xg for 15 min at 4 °C. 2 ml of the soluble lysate was incubated with 30 μl of anti-FLAG M2 affinity resins (Sigma-Aldrich) for 2 h at 4 °C. The protein-bound beads were washed five times with wash buffer [20 mM Tris-HCl (pH 8.0), 100 mM KCl, 5 mM $MgCl_2$, 10% glycerol, 0.1% NP-40, 1 mM DTT, 5 μg/ml leupeptin, 2 μg/ml aprotinin, 20 μg/ml trypsin inhibitor, 100 μg/ml PMSF] and stored in PBS at 4 °C. 10 μl of protein-bound FLAG beads were coupled with 100 μl of *Xenopus* egg extracts diluted five-fold by CPB containing 2% sucrose and incubated for 2 h at 4 °C. The beads were washed three times by CPB containing 2% sucrose and 0.1% Triton X-100, followed by resuspension by 10 μl of 2xLaemmli sample buffer and 20 μl of 1xLaemmli sample buffer.

Mass spectrometry

The eluted proteins were trypsin-digested, desalted using ZipTip C18 (Millipore) and centrifuged in a vacuum concentrator. Shotgun proteomic

664 analyses of the digested peptides were performed by LTQ-Orbitrap Velos mass
665 spectrometer (Thermo Fisher Scientific) coupled with Dina-2A nanoflow liquid
666 chromatography system (KYA Technologies). The samples were injected into a
667 75-μm reversed-phase C18 column at a flow rate of 10 μl/min and eluted with a
668 linear gradient of solvent A (2% acetonitrile and 0.1% formic acid in H_2O) to
669 solvent B (40% acetonitrile and 0.1% formic acid in H_2O) at 300 nl/min. Peptides
670 were sequentially sprayed from a nanoelectrospray ion source (KYA
671 Technologies) and analyzed by collision-induced dissociation (CID). The
672 analyses were operated in data-dependent mode, switching automatically
673 between MS and MS/MS acquisition. For CID analyses, full-scan MS spectra
674 (from m/z 380 to 2,000) were acquired in the orbitrap with a resolution of
675 100,000 at m/z 400 after ion count accumulation to the target value of 1,000,000.
676 The 20 most intense ions at a threshold above 2,000 were fragmented in the
677 linear ion trap with a normalized collision energy of 35% for an activation time
678 of 10 ms. The orbitrap analyzer was operated with the "lock mass" option to
679 perform shotgun detection with high accuracy. Protein identification was
680 conducted by searching MS and MS/MS data against NCBI (National Center for
681 Biotechnology Information) *Xenopus laevis* protein database using Mascot
682 (Matrix Science). Methionine oxidation, protein N-terminal acetylation and
683 pyro-glutamination for N-terminal glutamine were set as variable modifications.

A maximum of two missed cleavages was allowed in our database search, while the mass tolerance was set to three parts per million (ppm) for peptide masses and 0.8 Da for MS/MS peaks. In the process of peptide identification, we applied a filter to satisfy a false discovery rate lower than 1%. The mass spectrometry proteomics data have been deposited to the ProteomeXchange Consortium via the jPOST repository with the dataset identifier PXD034088.

In vitro deubiquitylation assay

Ubiquitylated PAF15, a substrate for the deubiquitylation assay, was prepared by *in vitro* ubiquitylation using recombinant mouse UBA1 (E1), human UBE2D3 (E2), human UHRF1 (E3), ubiquitin and PAF15. N-terminal six histidine tagged E1 was expressed in Sf9 cells using the baculo virus system according to the manufacture's instruction. The protein was purified by TALON affinity (Clontech), HiTrap-Q anion-exchange (Cytiva) and Hiload 26/600 S200 size-exclusion (Cytiva) chromatographies. E2 was expressed in *Escherichia coli* BL21 as a GST-fusion protein and purified by GS4B affinity (Cytiva) and d Hiload 26/600 S75 size-exclusion chromatographies (Cytiva). UHRF1 was expressed in *Escherichia coli* Rossetta2 and purified using GS4B affinity, HiTrap Heparin and Hiload 26/600 S200 size-exclusion

703 chromatographies. Ubiquitin was expressed in BL21 and purified using HiTrap
704 SP anion-exchange (Cytiva) and Hiload 26/600 S75 size-exclusion
705 chromatographies. PAF15 including C-terminal FLAG tag was expressed in
706 *Escherichia coli*, BL21 and purified GS4B affinity, HiTrap SP anion-exchange and
707 Hiload 26/600 S75 size-exclusion chromatographies. The ubiquitylation reaction
708 mixture contained 0.4 μM E1, 6 μM E2, 3 μM E3, 600 μM Ubiquitin, and 100 μM
709 PAF15 in a ubiquitylation reaction buffer [50 mM Tris-HCl (pH 8.0), 50 mM
710 NaCl, 5 mM $MgCl_2$, 0.1% Triton X-100, and 2 mM DTT]. The reaction mixture
711 was incubated at 25 °C for overnight.

712 For *in vitro* deubiquitylation assay, recombinant USP7 full-length wild-
713 type/C223A and deletion of TRAF domain were expressed in Rossetta2 and
714 purified by GST-affinity, HiTrap Q anion-exchange and Hiload 26/600 S200
715 size-exclusion chromatographies. 3.75 pmol (conc.: 50 nM) of USP7 or USP47
716 (R&D SYSTEMS, E-626-050) and the ubiquitylated PAF15 were incubated in 75
717 μl reaction solution in a reaction buffer [20 mM Tris-HCl (pH 7.5), 150 mM
718 NaCl, 0.5 mM DTT and 10% glycerol] at 20 °C for 1 hr. The reaction was
719 stopped at indicated times by adding SDS-sample buffer and the
720 deubiquitylation was analyzed by SDA-PAGE.

721

Recombinant proteins expression and purification

GST-PAF15, 3xFLAG-tagged PAF15, 3xFLAG-tagged DNMT1 WT and 4KA mutant, and GST-mDPPA3 61-150 mutant expression and purification were described previously (Mulholland et al., 2020; Nishiyama et al., 2020; Yamaguchi et al., 2017). S79A/S97A, K101A/K105A mutations in pGEX4T-3 and pKS104-PAF15 constructs were introduced using a KOD-Plus Mutagenesis Kit (Toyobo). These mutant x*PAF15* DNAs from pKS104-PAF15 were amplified by PCR and ligated into pVL1392 vector. *USP7 C225S* mutation was also introduced by KOD-Plus Mutagenesis Kit. GST-tagged protein expression in *Escherichia coli* (BL21-CodonPlus) was induced by the addition of 0.1 M Isopropyl-β-D-1-thiogalactopyranoside (IPTG) to media followed by incubation for 12 h at 20 °C. For purification of GST-tagged proteins, cells were collected and resuspended in lysis buffer [20 mM HEPES-KOH (pH 7.6), 0.5 M NaCl, 0.5 mM EDTA, 10% glycerol, 1 mM DTT] supplemented with 0.5% NP-40 and protease inhibitors and were then disrupted by sonication on ice. For FLAG-tagged protein expression in insect cells, 3xFLAG-tagged *USP7 WT* or mutants were transferred from pKS103 vector into pVL1392 vector. Baculoviruses were produced using a BD BaculoGold Transfection Kit and a BestBac Transfection Kit (BD Biosciences), following the manufacturer's protocol. Proteins were expressed in Sf9 insect cells by infection with viruses expressing 3xFLAG-

742 tagged PAF15 WT or its mutants for 72 h at 27 °C. Sf9 cells from a 750 ml
743 culture were collected and lysed by resuspending them in 30 ml lysis buffer,
744 followed by incubation on ice for 10 min. A soluble fraction was obtained after
745 centrifugation of the lysate at 15,000 xg for 15 min at 4 °C. The soluble fraction
746 was incubated for 4 h at 4 °C with 250 μl of anti-FLAG M2 affinity resin
747 equilibrated with lysis buffer. The beads were collected and washed with 10 ml
748 wash buffer and then with 5 ml of EB [20 mM HEPES-KOH (pH 7.5), 100 mM
749 KCl, 5 mM $MgCl_2$] containing 1 mM DTT. Each recombinant protein was eluted
750 twice in 250 μl of EB containing 1 mM DTT and 250 μg/ml 3xFLAG peptide
751 (Sigma-Aldrich). Eluates were pooled and concentrated using a Vivaspin 500
752 (GE Healthcare).

753 The human ATAD5-RFC-like complex (ATAD5-RLC) was expressed
754 and purified as follows. Human 293T cells (5 x 10^6 cells) cultured in a 15 cm
755 dish were transfected with 8 μg of the human mini-AzamiGreen-tagged *ATAD5*
756 gene, and 1 μg each of untagged *RFC2*, *RFC3*, *RFC4*, and *RFC5* genes, all
757 inserted into the pCSII-EF vector, and incubated for 72 h in D-MEM (Sigma-
758 Aldrich) supplemented with 10% fetal bovine serum at 37°C. Cells from ten
759 dishes were harvested, resuspended in 8 ml of PBSGE [140 mM NaCl, 2.7 mM
760 KCl, 10 mM Na_2HPO_4, 1.7 mM NaH_2PO_4, 20% glycerol, and 20 μM EDTA]
761 supplemented with 1 mM PMSF and 20 μg/ml leupeptin, and lysed by the

addition of 0.5% NP-40. The lysates were incubated on ice for 10 min, supplemented with final 0.5 M NaCl, and clarified by centrifugation at 75,000 xg for 30 min at 4 °C. Cleared lysates were then applied onto 1 ml anti-FLAG M2 affinity resin packed in a column equilibrated with PC buffer [50 mM KPO_4 (pH 7.5), 0.5 mM EDTA, 1 mM 3-[(3-Cholamidopropyl)dimethylammonio]propanesulfonate (CHAPS) and 10% glycerol] supplemented with 0.5 M NaCl. The column was washed with PC buffer supplemented with 0.5 M NaCl, and the ATAD5-RLC proteins were eluted with 100 μg/mL FLAG-peptide (Sigma Aldrich) in the same buffer. Peak fractions were collected and used for the assay.

Quantification of DNA replication and DNA methylation efficiency in *Xenopus* egg extracts

[α-^{32}P] dCTP (3,000 Ci/mmol) and sperm nuclei were added to interphase extracts and incubated at 22 °C. At each time point, extracts were diluted in reaction stop solution (1% SDS, 40 mM EDTA) and treated with Proteinase K (NACALAI TESQUE, Inc.) at 37 °C. The solutions were spotted onto Whatman glass microfiber filters followed by 5% trichloroacetic acid (TCA) containing 2% pyrophosphate. Filters were washed twice in ethanol and

781 dried. The incorporation of radioactivity was counted in the scintillation
782 cocktail. DNA methylation was monitored by the incorporation of S-[methyl-
783 ^{3}H]-adenosyl-L-methionine. Extracts supplemented with S-[methyl-^{3}H]-
784 adenosyl-L-methionine and sperm nuclei were incubated at 22 °C. At each time
785 point, the reaction was stopped by dilution in CPB containing 2% sucrose up to
786 300 μl. Genomic DNA was purified using a Wizard Genomic DNA Purification
787 Kit (Promega). Incorporation of radioactivity was counted in the scintillation
788 cocktail.

789

790 **Immunoprecipitation from chromatin lysate**

791 MNase-digested chromatin fractions were prepared as described
792 previously (Nishiyama et al., 2020). The chromatin pellet was resuspended and
793 digested in 100 μl of digestion buffer [10 mM HEPES-KOH (pH 7.5), 50 mM
794 KCl, 2.5 mM $MgCl_2$, 0.1 mM $CaCl_2$, 0.1% Triton X-100, 2 mM NEM, 100 μM PR-
795 619] containing 4 U/ml MNase at 22 °C for 20 min. The reaction was stopped by
796 the addition of 10 mM EDTA, and the solution was centrifuged at 17,700 xg for
797 10 min. For the immunoprecipitation experiment, 2 μg purified IgG, PAF15,
798 USP7 or DNMT1 antibodies were bound to 10 μl of Protein A agarose beads
799 and these beads were mixed with digested chromatin lysates at 4 °C for 2 h.

After reaction, these beads were washed by CPB containing 2% sucrose and 0.1% Triton X-100 and resuspended in 10 μl of 2xLaemmli buffer and 20 μl of 1xLaemmli buffer, heated at 100 °C.

Statistical analysis

Statistics

The normal distribution of the population at the 0.05 level was calculated using the Shapiro-Wilk normality test. Data are presented as mean ± SEM, unless otherwise noted. Multiple comparisons were performed by Two-way Repeated Measure analysis of variance (RM ANOVA) followed by Sidak's multiple comparison test. For consistency of comparison, significance in all Figures is indicated as follows. ◎p < 0.05, ◎◎p < 0.01, ◎◎◎p < 0.001, ◎◎◎◎p < 0.0001.

Data availability

All data generated or analysed during this study are included in the manuscript and supporting files; source data files for all figures have been provided.

Acknowledgement

We thank Chikahide Masutani for human USP7 antibodies. The study

820 is funded by MEXT/JSPS KAKENHI (JP19H05740 to M.N.; JP19H03143 and
821 JP19H05285 to A.N.; JP16H06578 to M.O.). A.N. was supported in part by a
822 grant from Daiichi Sankyo Foundation of Life Science.

823

824 Competing interests

825 The authors declare no competing interests.

826

827 References

828 Arita, K., Ariyoshi, M., Tochio, H., Nakamura, Y., & Shirakawa, M. (2008).
829 Recognition of hemi-methylated DNA by the SRA protein UHRF1 by a
830 base-flipping mechanism. *Nature*, *455*(7214), 818-821.
831 https://doi.org/10.1038/nature07249

832 Arita, K., Isogai, S., Oda, T., Unoki, M., Sugita, K., Sekiyama, N., Kuwata, K.,
833 Hamamoto, R., Tochio, H., Sato, M., Ariyoshi, M., & Shirakawa, M.
834 (2012). Recognition of modification status on a histone H3 tail by linked
835 histone reader modules of the epigenetic regulator UHRF1. *Proc Natl*
836 *Acad Sci U S A*, *109*(32), 12950-12955.
837 https://doi.org/10.1073/pnas.1203701109

838 Ashton, N. W., Valles, G. J., Jaiswal, N., Bezsonova, I., & Woodgate, R. (2021).
839 DNA Polymerase iota Interacts with Both the TRAF-like and UBL1-2

840 Domains of USP7. *J Mol Biol*, *433*(2), 166733.
841 https://doi.org/10.1016/j.jmb.2020.166733

842 Avvakumov, G. V., Walker, J. R., Xue, S., Li, Y., Duan, S., Bronner, C.,
843 Arrowsmith, C. H., & Dhe-Paganon, S. (2008). Structural basis for
844 recognition of hemi-methylated DNA by the SRA domain of human
845 UHRF1. *Nature*, *455*(7214), 822-825. https://doi.org/10.1038/nature07273

846 Blow, J. J., & Laskey, R. A. (2016). Xenopus cell-free extracts and their
847 contribution to the study of DNA replication and other complex
848 biological processes. *Int J Dev Biol*, *60*(7-8-9), 201-207.
849 https://doi.org/10.1387/ijdb.160142jb

850 Borodovsky, A., Kessler, B. M., Casagrande, R., Overkleeft, H. S., Wilkinson, K.
851 D., & Ploegh, H. L. (2001). A novel active site-directed probe speci®c
852 fordeubiquitylating enzymes reveals proteasomeassociation of USP14.
853 *EMBO J.*, *20*(18), 5187-5196. https://doi.org/10.1093/emboj/20.18.5187

854 Bostick, M., Jong, K. K., Estève, P. O., Clark, A., Pradhan, S., & Jacobsen, S. E.
855 (2007). HRF1 plays a role in maintaining DNA methylation in
856 mammalian cells. *Science*, *317*(5845), 1760-1764.
857 https://doi.org/10.1126/science.1147939

858 Cheng, J., Li, Z., Gong, R., Fang, J., Yang, Y., Sun, C., Yang, H., & Xu, Y. (2015).
859 Molecular mechanism for the substrate recognition of USP7. *Protein Cell*,

6(11), 849-852. https://doi.org/10.1007/s13238-015-0192-y

Cheng, J., Yang, H., Fang, J., Ma, L., Gong, R., Wang, P., Li, Z., & Xu, Y. (2015). Molecular mechanism for USP7-mediated DNMT1 stabilization by acetylation. *Nat Commun*, *6*, 7023. https://doi.org/10.1038/ncomms8023

DaRosa, P. A., Harrison, J. S., Zelter, A., Davis, T. N., Brzovic, P., Kuhlman, B., & Klevit, R. E. (2018). A Bifunctional Role for the UHRF1 UBL Domain in the Control of Hemi-methylated DNA-Dependent Histone Ubiquitylation. *Mol Cell*, *72*(4), 753-765 e756. https://doi.org/10.1016/j.molcel.2018.09.029

De Biasio, A., de Opakua, A. I., Mortuza, G. B., Molina, R., Cordeiro, T. N., Castillo, F., Villate, M., Merino, N., Delgado, S., Gil-Carton, D., Luque, I., Diercks, T., Bernado, P., Montoya, G., & Blanco, F. J. (2015). Structure of p15(PAF)-PCNA complex and implications for clamp sliding during DNA replication and repair. *Nat Commun*, *6*, 6439. https://doi.org/10.1038/ncomms7439

Dimova, N. V., Hathaway, N. A., Lee, B. H., Kirkpatrick, D. S., Berkowitz, M. L., Gygi, S. P., Finley, D., & King, R. W. (2012). APC/C-mediated multiple monoubiquitylation provides an alternative degradation signal for cyclin B1. *Nat Cell Biol*, *14*(2), 168-176. https://doi.org/10.1038/ncb2425

Du, W., Dong, Q., Zhang, Z., Liu, B., Zhou, T., Xu, R. M., Wang, H., Zhu, B., &

Li, Y. (2019). Stella protein facilitates DNA demethylation by disrupting the chromatin association of the RING finger-type E3 ubiquitin ligase UHRF1. *J Biol Chem*, *294*(22), 8907-8917. https://doi.org/10.1074/jbc.RA119.008008

Du, Z., Song, J., Wang, Y., Zhao, Y., Guda, K., Yang, S., Kao, H. Y., Xu, Y., Willis, J., Markowitz, S. D., Sedwick, D., Ewing, R. M., & Wang, Z. (2010). DNMT1 stability is regulated by proteins coordinating deubiquitination and acetylation-driven ubiquitination. *Sci. Signal.*, *3*(146), ra80. https://doi.org/10.1126/scisignal.2001462

Edwards, J. R., Yarychkivska, O., Boulard, M., & Bestor, T. H. (2017). DNA methylation and DNA methyltransferases. *Epigenetics Chromatin*, *10*, 23. https://doi.org/10.1186/s13072-017-0130-8

Emanuele, M. J., Ciccia, A., Elia, A. E., & Elledge, S. J. (2011). Proliferating cell nuclear antigen (PCNA)-associated KIAA0101/PAF15 protein is a cell cycle-regulated anaphase-promoting complex/cyclosome substrate. *Proc Natl Acad Sci U S A*, *108*(24), 9845-9850. https://doi.org/10.1073/pnas.1106136108

Felle, M., Joppien, S., Nemeth, A., Diermeier, S., Thalhammer, V., Dobner, T., Kremmer, E., Kappler, R., & Langst, G. (2011). The USP7/Dnmt1 complex stimulates the DNA methylation activity of Dnmt1 and regulates the

stability of UHRF1. *Nucleic Acids Res*, *39*(19), 8355-8365. https://doi.org/10.1093/nar/gkr528

Foster, B. M., Stolz, P., Mulholland, C. B., Montoya, A., Kramer, H., Bultmann, S., & Bartke, T. (2018). Critical Role of the UBL Domain in Stimulating the E3 Ubiquitin Ligase Activity of UHRF1 toward Chromatin. *Mol Cell*, *72*(4), 739-752 e739. https://doi.org/10.1016/j.molcel.2018.09.028

Georges, A., Coyaud, E., Marcon, E., Greenblatt, J., Raught, B., & Frappier, L. (2019). USP7 Regulates Cytokinesis through FBXO38 and KIF20B. *Sci Rep*, *9*(1), 2724. https://doi.org/10.1038/s41598-019-39368-y

Greenberg, M. V. C., & Bourc'his, D. (2019). The diverse roles of DNA methylation in mammalian development and disease. *Nat Rev Mol Cell Biol*, *20*(10), 590-607. https://doi.org/10.1038/s41580-019-0159-6

Haggerty, C., Kretzmer, H., Riemenschneider, C., Kumar, A. S., Mattei, A. L., Bailly, N., Gottfreund, J., Giesselmann, P., Weigert, R., Brandl, B., Giehr, P., Buschow, R., Galonska, C., von Meyenn, F., Pappalardi, M. B., McCabe, M. T., Wittler, L., Giesecke-Thiel, C., Mielke, T., Meierhofer, D., Timmermann, B., Muller, F. J., Walter, J., & Meissner, A. (2021). Dnmt1 has de novo activity targeted to transposable elements. *Nat Struct Mol Biol*, *28*(7), 594-603. https://doi.org/10.1038/s41594-021-00603-8

Harrison, J. S., Cornett, E. M., Goldfarb, D., DaRosa, P. A., Li, Z. M., Yan, F.,

Dickson, B. M., Guo, A. H., Cantu, D. V., Kaustov, L., Brown, P. J., Arrowsmith, C. H., Erie, D. A., Major, M. B., Klevit, R. E., Krajewski, K., Kuhlman, B., Strahl, B. D., & Rothbart, S. B. (2016). Hemi-methylated DNA regulates DNA methylation inheritance through allosteric activation of H3 ubiquitylation by UHRF1. *Elife*, *5*. https://doi.org/10.7554/eLife.17101

Hashimoto, H., Horton, J. R., Zhang, X., Bostick, M., Jacobsen, S. E., & Cheng, X. (2008). The SRA domain of UHRF1 flips 5-methylcytosine out of the DNA helix. *Nature*, *455*(7214), 826-829. https://doi.org/10.1038/nature07280

Hu, M., Gu, L., Li, M., Jeffrey, P. D., Gu, W., & Shi, Y. (2006). Structural basis of competitive recognition of p53 and MDM2 by HAUSP/USP7: implications for the regulation of the p53-MDM2 pathway. *PLoS Biol*, *4*(2), e27. https://doi.org/10.1371/journal.pbio.0040027

Hu, M., Li, P., Li, M., Li, W., Yao, T., Wu, J. W., Gu, W., Cohen, R. E., & Shi, Y. (2002). Crystal Structure of a UBP-Family Deubiquitinating. *Cell 111*(7), 1041-1054. https://doi.org/10.1016/S0092-8674(02)01199-6

Ishiyama, S., Nishiyama, A., Saeki, Y., Moritsugu, K., Morimoto, D., Yamaguchi, L., Arai, N., Matsumura, R., Kawakami, T., Mishima, Y., Hojo, H., Shimamura, S., Ishikawa, F., Tajima, S., Tanaka, K., Ariyoshi,

940 M., Shirakawa, M., Ikeguchi, M., Kidera, A., Suetake, I., Arita, K., &
941 Nakanishi, M. (2017). Structure of the Dnmt1 Reader Module Complexed
942 with a Unique Two-Mono-Ubiquitin Mark on Histone H3 Reveals the
943 Basis for DNA Methylation Maintenance. *Mol Cell*, *68*(2), 350-360 e357.
944 https://doi.org/10.1016/j.molcel.2017.09.037
945 Jagannathan, M., Nguyen, T., Gallo, D., Luthra, N., Brown, G. W., Saridakis, V.,
946 & Frappier, L. (2014). A role for USP7 in DNA replication. *Mol Cell Biol*,
947 *34*(1), 132-145. https://doi.org/10.1128/MCB.00639-13
948 Johnson, C., Gali, V. K., Takahashi, T. S., & Kubota, T. (2016). PCNA Retention
949 on DNA into G2/M Phase Causes Genome Instability in Cells Lacking
950 Elg1. *Cell Rep*, *16*(3), 684-695. https://doi.org/10.1016/j.celrep.2016.06.030
951 Jones, P. A. (2012). Functions of DNA methylation: islands, start sites, gene
952 bodies and beyond. *Nat Rev Genet*, *13*(7), 484-492.
953 https://doi.org/10.1038/nrg3230
954 Jones, P. A., & Liang, G. (2009). Rethinking how DNA methylation patterns are
955 maintained. *Nat Rev Genet*, *10*(11), 805-811.
956 https://doi.org/10.1038/nrg2651
957 Kang, M. S., Ryu, E., Lee, S. W., Park, J., Ha, N. Y., Ra, J. S., Kim, Y. J., Kim, J.,
958 Abdel-Rahman, M., Park, S. H., Lee, K. Y., Kim, H., Kang, S., & Myung,
959 K. (2019). Regulation of PCNA cycling on replicating DNA by RFC and

960 RFC-like complexes. *Nat Commun*, *10*(1), 2420.
961 https://doi.org/10.1038/s41467-019-10376-w

962 Karg, E., Smets, M., Ryan, J., Forne, I., Qin, W., Mulholland, C. B., Kalideris, G.,
963 Imhof, A., Bultmann, S., & Leonhardt, H. (2017). Ubiquitome Analysis
964 Reveals PCNA-Associated Factor 15 (PAF15) as a Specific Ubiquitination
965 Target of UHRF1 in Embryonic Stem Cells. *J Mol Biol*, *429*(24), 3814-3824.
966 https://doi.org/10.1016/j.jmb.2017.10.014

967 Komander, D., & Rape, M. (2012). The ubiquitin code. *Annu Rev Biochem*, *81*,
968 203-229. https://doi.org/10.1146/annurev-biochem-060310-170328

969 Kubota, T., Katou, Y., Nakato, R., Shirahige, K., & Donaldson, A. D. (2015).
970 Replication-Coupled PCNA Unloading by the Elg1 Complex Occurs
971 Genome-wide and Requires Okazaki Fragment Ligation. *Cell Rep*, *12*(5),
972 774-787. https://doi.org/10.1016/j.celrep.2015.06.066

973 Kubota, T., Nishimura, K., Kanemaki, M. T., & Donaldson, A. D. (2013). The
974 Elg1 replication factor C-like complex functions in PCNA unloading
975 during DNA replication. *Mol Cell*, *50*(2), 273-280.
976 https://doi.org/10.1016/j.molcel.2013.02.012

977 Kumamoto, S., Nishiyama, A., Chiba, Y., Miyashita, R., Konishi, C., Azuma, Y.,
978 & Nakanishi, M. (2021). HPF1-dependent PARP activation promotes
979 LIG3-XRCC1-mediated backup pathway of Okazaki fragment ligation.

Nucleic Acids Res, *49*(9), 5003-5016. https://doi.org/10.1093/nar/gkab269

Landre, V., Revi, B., Mir, M. G., Verma, C., Hupp, T. R., Gilbert, N., & Ball, K. L. (2017). Regulation of transcriptional activators by DNA-binding domain ubiquitination. *Cell Death Differ*, *24*(5), 903-916. https://doi.org/10.1038/cdd.2017.42

Lee, K. Y., Fu, H., Aladjem, M. I., & Myung, K. (2013). ATAD5 regulates the lifespan of DNA replication factories by modulating PCNA level on the chromatin. *J Cell Biol*, *200*(1), 31-44. https://doi.org/10.1083/jcb.201206084

Li, J., Wang, R., Jin, J., Han, M., Chen, Z., Gao, Y., Hu, X., Zhu, H., Gao, H., Lu, K., Shao, Y., Lyu, C., Lai, W., Li, P., Hu, G., Li, J., Li, D., Wang, H., Wu, Q., & Wong, J. (2020). USP7 negatively controls global DNA methylation by attenuating ubiquitinated histone-dependent DNMT1 recruitment. *Cell Discov*, *6*, 58. https://doi.org/10.1038/s41421-020-00188-4

Li, M., Chen, D., Shiloh, A., Luo, J., Nikolaev, Y. A., Qin, J., & Gu, W. (2002). Deubiquitination of p53 by HAUSP is an important pathway for p53 stabilization. *Nature*, *416*(6881), 644-648. https://doi.org/10.1038/nature735

Li, Y., Zhang, Z., Chen, J., Liu, W., Lai, W., Liu, B., Li, X., Liu, L., Xu, S., Dong, Q., Wang, M., Duan, X., Tan, J., Zheng, Y., Zhang, P., Fan, G., Wong, J., Xu, G. L., Wang, Z., Wang, H., Gao, S., & Zhu, B. (2018). Stella safeguards the oocyte methylome by preventing de novo methylation mediated by

DNMT1. *Nature*, *564*(7734), 136-140. https://doi.org/10.1038/s41586-018-0751-5

Liu, P., Gan, W., Su, S., Hauenstein, A. V., Fu, T. M., Brasher, B., Schwerdtfeger, C., Liang, A. C., Xu, M., & Wei, W. (2018). K63-linked polyubiquitin chains bind to DNA to facilitate DNA damage repair. *Sci Signal*, *11*(533). https://doi.org/10.1126/scisignal.aar8133

Lyko, F. (2018). The DNA methyltransferase family: a versatile toolkit for epigenetic regulation. *Nat Rev Genet*, *19*(2), 81-92. https://doi.org/10.1038/nrg.2017.80

Ma, H., Chen, H., Guo, X., Wang, Z., Sowa, M. E., Zheng, L., Hu, S., Zeng, P., Guo, R., Diao, J., Lan, F., Harper, J. W., Shi, Y. G., Xu, Y., & Shi, Y. (2012). M phase phosphorylation of the epigenetic regulator UHRF1 regulates its physical association with the deubiquitylase USP7 and stability. *Proc Natl Acad Sci U S A*, *109*(13), 4828-4833. https://doi.org/10.1073/pnas.1116349109

Ming, X., Zhang, Z., Zou, Z., Lv, C., Dong, Q., He, Q., Yi, Y., Li, Y., Wang, H., & Zhu, B. (2020). Kinetics and mechanisms of mitotic inheritance of DNA methylation and their roles in aging-associated methylome deterioration. *Cell Res*, *30*(11), 980-996. https://doi.org/10.1038/s41422-020-0359-9

Mishima, Y., Brueckner, L., Takahashi, S., Kawakami, T., Otani, J., Shinohara,

A., Takeshita, K., Garvilles, R. G., Watanabe, M., Sakai, N., Takeshima, H., Nachtegael, C., Nishiyama, A., Nakanishi, M., Arita, K., Nakashima, K., Hojo, H., & Suetake, I. (2020). Enhanced processivity of Dnmt1 by monoubiquitinated histone H3. *Genes Cells*, *25*(1), 22-32. https://doi.org/10.1111/gtc.12732

Moore, L. D., Le, T., & Fan, G. (2013). DNA methylation and its basic function. *Neuropsychopharmacology*, *38*(1), 23-38. https://doi.org/10.1038/npp.2012.112

Mulholland, C. B., Nishiyama, A., Ryan, J., Nakamura, R., Yigit, M., Gluck, I. M., Trummer, C., Qin, W., Bartoschek, M. D., Traube, F. R., Parsa, E., Ugur, E., Modic, M., Acharya, A., Stolz, P., Ziegenhain, C., Wierer, M., Enard, W., Carell, T., Lamb, D. C., Takeda, H., Nakanishi, M., Bultmann, S., & Leonhardt, H. (2020). Recent evolution of a TET-controlled and DPPA3/STELLA-driven pathway of passive DNA demethylation in mammals. *Nat Commun*, *11*(1), 5972. https://doi.org/10.1038/s41467-020-19603-1

Nishiyama, A., Mulholland, C. B., Bultmann, S., Kori, S., Endo, A., Saeki, Y., Qin, W., Trummer, C., Chiba, Y., Yokoyama, H., Kumamoto, S., Kawakami, T., Hojo, H., Nagae, G., Aburatani, H., Tanaka, K., Arita, K., Leonhardt, H., & Nakanishi, M. (2020). Two distinct modes of DNMT1

recruitment ensure stable maintenance DNA methylation. *Nat Commun*, *11*(1), 1222. https://doi.org/10.1038/s41467-020-15006-4

Nishiyama, A., Yamaguchi, L., Sharif, J., Johmura, Y., Kawamura, T., Nakanishi, K., Shimamura, S., Arita, K., Kodama, T., Ishikawa, F., Koseki, H., & Nakanishi, M. (2013). Uhrf1-dependent H3K23 ubiquitylation couples maintenance DNA methylation and replication. *Nature*, *502*(7470), 249-253. https://doi.org/10.1038/nature12488

Petryk, N., Bultmann, S., Bartke, T., & Defossez, P. A. (2021). Staying true to yourself: mechanisms of DNA methylation maintenance in mammals. *Nucleic Acids Res*, *49*(6), 3020-3032. https://doi.org/10.1093/nar/gkaa1154

Povlsen, L. K., Beli, P., Wagner, S. A., Poulsen, S. L., Sylvestersen, K. B., Poulsen, J. W., Nielsen, M. L., Bekker-Jensen, S., Mailand, N., & Choudhary, C. (2012). Systems-wide analysis of ubiquitylation dynamics reveals a key role for PAF15 ubiquitylation in DNA-damage bypass. *Nat Cell Biol*, *14*(10), 1089-1098. https://doi.org/10.1038/ncb2579

Qin, W., Leonhardt, H., & Spada, F. (2011). Usp7 and Uhrf1 control ubiquitination and stability of the maintenance DNA methyltransferase Dnmt1. *J Cell Biochem*, *112*(2), 439-444. https://doi.org/10.1002/jcb.22998

Qin, W., Wolf, P., Liu, N., Link, S., Smets, M., La Mastra, F., Forne, I., Pichler, G., Horl, D., Fellinger, K., Spada, F., Bonapace, I. M., Imhof, A., Harz, H., &

Leonhardt, H. (2015). DNA methylation requires a DNMT1 ubiquitin interacting motif (UIM) and histone ubiquitination. *Cell Res*, *25*(8), 911-929. https://doi.org/10.1038/cr.2015.72

Rajakumara, E., Wang, Z., Ma, H., Hu, L., Chen, H., Lin, Y., Guo, R., Wu, F., Li, H., Lan, F., Shi, Y. G., Xu, Y., Patel, D. J., & Shi, Y. (2011). PHD finger recognition of unmodified histone H3R2 links UHRF1 to regulation of euchromatic gene expression. *Mol Cell*, *43*(2), 275-284. https://doi.org/10.1016/j.molcel.2011.07.006

Ren, W., Fan, H., Grimm, S. A., Kim, J. J., Li, L., Guo, Y., Petell, C. J., Tan, X. F., Zhang, Z. M., Coan, J. P., Yin, J., Kim, D. I., Gao, L., Cai, L., Khudaverdyan, N., Cetin, B., Patel, D. J., Wang, Y., Cui, Q., Strahl, B. D., Gozani, O., Miller, K. M., O'Leary, S. E., Wade, P. A., Wang, G. G., & Song, J. (2021). DNMT1 reads heterochromatic H4K20me3 to reinforce LINE-1 DNA methylation. *Nat Commun*, *12*(1), 2490. https://doi.org/10.1038/s41467-021-22665-4

Rothbart, S. B., Krajewski, K., Nady, N., Tempel, W., Xue, S., Badeaux, A. I., Barsyte-Lovejoy, D., Martinez, J. Y., Bedford, M. T., Fuchs, S. M., Arrowsmith, C. H., & Strahl, B. D. (2012). Association of UHRF1 with methylated H3K9 directs the maintenance of DNA methylation. *Nat Struct Mol Biol*, *19*(11), 1155-1160. https://doi.org/10.1038/nsmb.2391

1080 Sharif, J., Muto, M., Takebayashi, S., Suetake, I., Iwamatsu, A., Endo, T. A.,
1081 Shinga, J., Mizutani-Koseki, Y., Toyoda, T., Okamura, K., Tajima, S.,
1082 Mitsuya, K., Okano, M., & Koseki, H. (2007). The SRA protein Np95
1083 mediates epigenetic inheritance by recruiting Dnmt1 to methylated
1084 DNA. *Nature*, *450*(7171), 908-912. https://doi.org/10.1038/nature06397
1085 Sheng, Y., Saridakis, V., Sarkari, F., Duan, S., Wu, T., Arrowsmith, C. H., &
1086 Frappier, L. (2006). Molecular recognition of p53 and MDM2 by
1087 USP7/HAUSP. *Nat Struct Mol Biol*, *13*(3), 285-291.
1088 https://doi.org/10.1038/nsmb1067
1089 Syeda, F., Fagan, R. L., Wean, M., Avvakumov, G. V., Walker, J. R., Xue, S., Dhe-
1090 Paganon, S., & Brenner, C. (2011). The replication focus targeting
1091 sequence (RFTS) domain is a DNA-competitive inhibitor of Dnmt1. *J Biol*
1092 *Chem*, *286*(17), 15344-15351. https://doi.org/10.1074/jbc.M110.209882
1093 Takebayashi, S., Tamura, T., Matsuoka, C., & Okano, M. (2007). Major and
1094 essential role for the DNA methylation mark in mouse embryogenesis
1095 and stable association of DNMT1 with newly replicated regions. *Mol Cell*
1096 *Biol*, *27*(23), 8243-8258. https://doi.org/10.1128/MCB.00899-07
1097 Takeshita, K., Suetake, I., Yamashita, E., Suga, M., Narita, H., Nakagawa, A., &
1098 Tajima, S. (2011). Structural insight into maintenance methylation by
1099 mouse DNA methyltransferase 1 (Dnmt1). *Proc Natl Acad Sci U S A*,

108(22), 9055-9059. https://doi.org/10.1073/pnas.1019629108

Ulrich, H. D. (2013). New insights into replication clamp unloading. *J Mol Biol*, *425*(23), 4727-4732. https://doi.org/10.1016/j.jmb.2013.05.003

Wang, Q., Yu, G., Ming, X., Xia, W., Xu, X., Zhang, Y., Zhang, W., Li, Y., Huang, C., Xie, H., Zhu, B., & Xie, W. (2020). Imprecise DNMT1 activity coupled with neighbor-guided correction enables robust yet flexible epigenetic inheritance. *Nat Genet*, *52*(8), 828-839. https://doi.org/10.1038/s41588-020-0661-y

Wyszynski, M. W., Gabbara, S., Kubareva, E. A., Romanova, E. A., Oretskaya, T. S., Gromova, E. S., Shabarova, Z. A., & Bhagwat, A. S. (1993). The cysteine conserved among DNA cytosine methylases is required for methyl transfer, but not for specific DNA binding.. *Nucleic Acids Res.*, *21*(2), 295-301. https://doi.org/10.1093/nar/21.2.295

Yamaguchi, L., Nishiyama, A., Misaki, T., Johmura, Y., Ueda, J., Arita, K., Nagao, K., Obuse, C., & Nakanishi, M. (2017). Usp7-dependent histone H3 deubiquitylation regulates maintenance of DNA methylation. *Sci Rep*, *7*(1), 55. https://doi.org/10.1038/s41598-017-00136-5

Yu, P., Huang, B., Shen, M., Lau, C., Chan, E., Michel, J., Xiong, Y., Payan, D. G., & Luo, Y. (2001). p15PAF, a novel PCNA associated factor with increased expression in. *Oncogene*(20), 484-489.

https://doi.org/10.1038/sj.onc.1204113

Zhang, Z. M., Liu, S., Lin, K., Luo, Y., Perry, J. J., Wang, Y., & Song, J. (2015). Crystal Structure of Human DNA Methyltransferase 1. *J Mol Biol*, *427*(15), 2520-2531. https://doi.org/10.1016/j.jmb.2015.06.001

Zhang, Z. M., Rothbart, S. B., Allison, D. F., Cai, Q., Harrison, J. S., Li, L., Wang, Y., Strahl, B. D., Wang, G. G., & Song, J. (2015). An Allosteric Interaction Links USP7 to Deubiquitination and Chromatin Targeting of UHRF1. *Cell Rep*, *12*(9), 1400-1406. https://doi.org/10.1016/j.celrep.2015.07.046

1130 Supplementary Figures

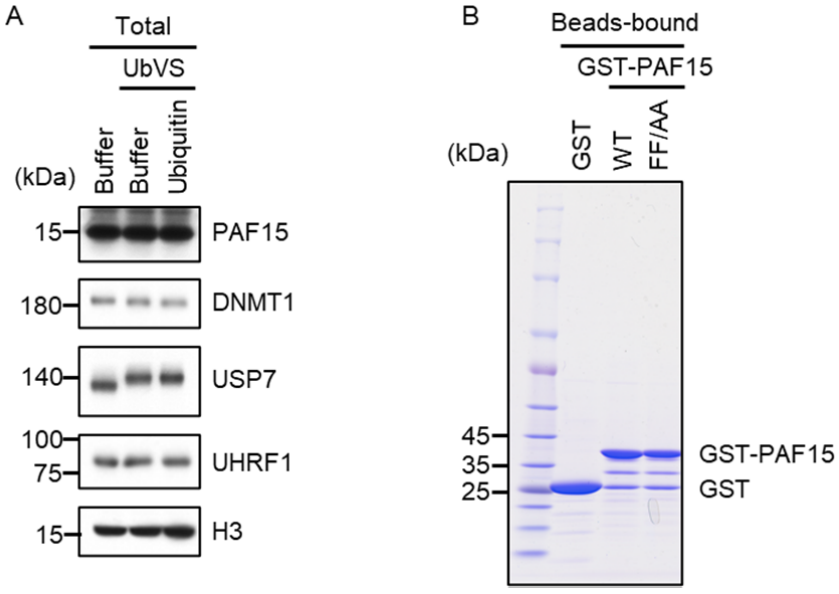

1131

1132 Supplemental Figure. S1 (A) Interphase egg extracts supplemented with UbVS

1133 or UbVS+Ub used in Figure 1A were analyzed by immunoblotting using the

1134 antibodies indicated. (B) Purified GST or GST-rPAF15 mutants used in Figure

1135 1D were stained using CBB. Source Data are provided as Figure S1-source data.

1136

1137

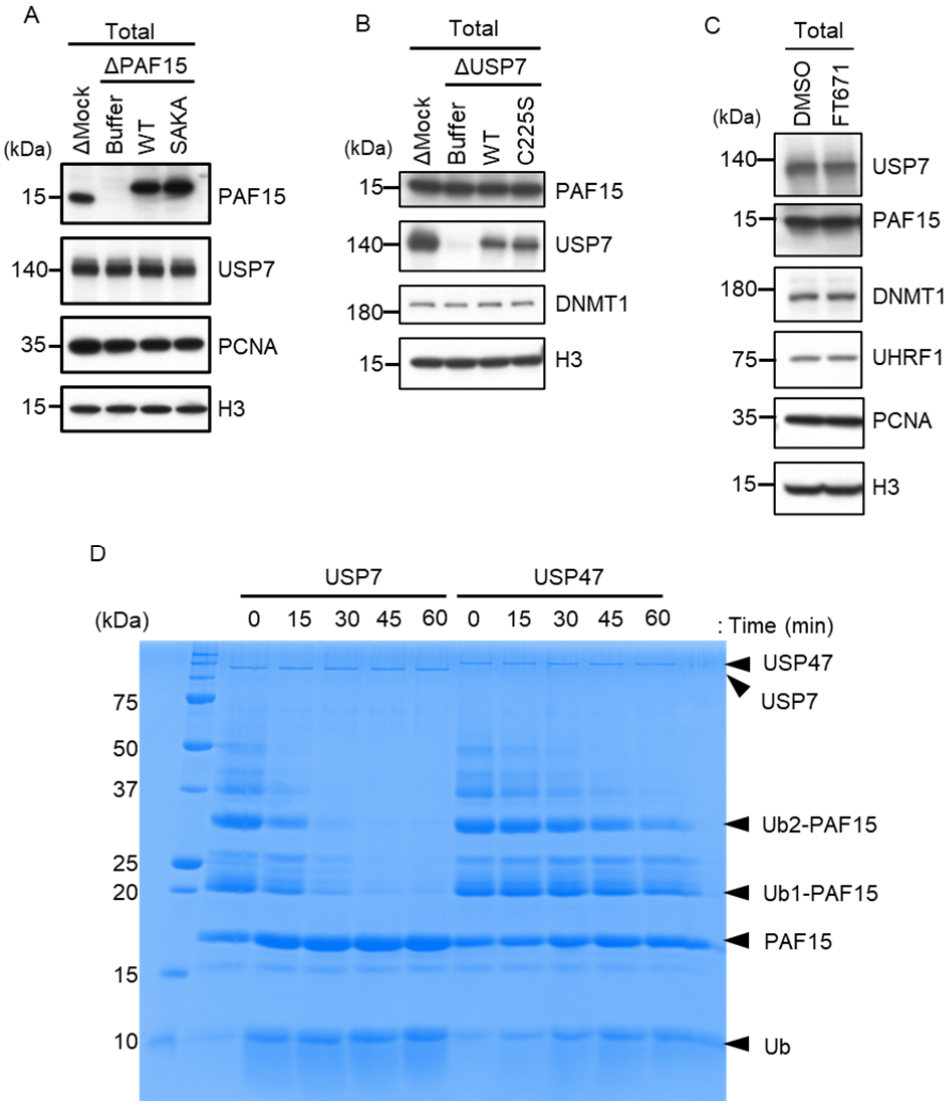

1138

1139

Supplemental Figure. S2 (A) rPAF15 WT-3xFLAG or SAKA-3xFLAG were added to PAF15-depleted extracts. The extracts used in Figure 3A were analyzed by immunoblotting using the antibodies indicated. (B) rUSP7 WT-3xFLAG or C225S-3xFLAG were added to USP7-depleted extracts. The extracts used in Figure 3B were analyzed by immunoblotting using the antibodies indicated. (C) Interphase egg extracts supplemented with Dimethyl sulfoxide (DMSO) or the USP7 inhibitor FT671 used in Figure 3C were analyzed by immunoblotting using the antibodies indicated. (D) Ubiquitinated PAF15 was prepared by *in vitro* ubiquitylation using E1 (mouse UBA1), E2 (UBE2D3), E3 (UHRF1), ubiquitin and C-teminal FLAG tagged PAF15. The reaction mixture was boiled and the precipitant was removed by centrifugation. The supernatant containing ubiquitinated PAF15 was incubated with 50 nM recombinant USP7 or USP47. Incubations were stopped at the indicated time by adding SDS-PAGE loading buffer and analyzed by CBB staining. Source Data are provided as Figure S2-source data.

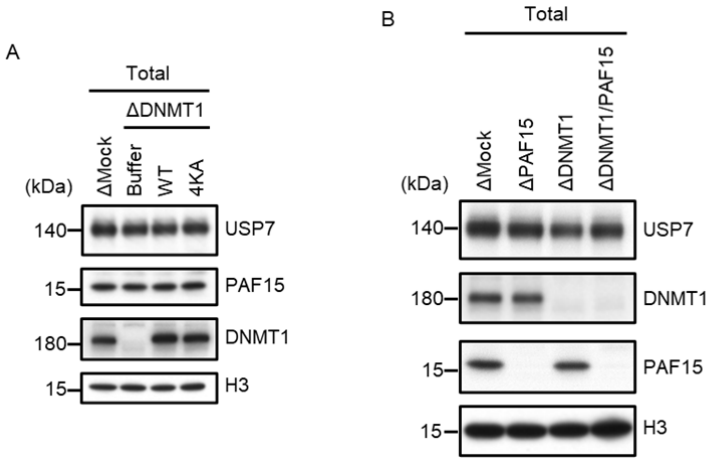

Supplemental Figure. S3 (A) rDNMT1WT-3xFLAG or 4KA-3xFLAG were added to DNMT1-depleted extracts. The extracts used in Figure 4C were analyzed by immunoblotting using the antibodies indicated. (B) Mock-, PAF15-, DNMT1- or PAF15/DNMT1 co-depleted extracts used in Figure 4D were analyzed by immunoblotting using the antibodies indicated. Source Data are provided as Figure S3-source data.

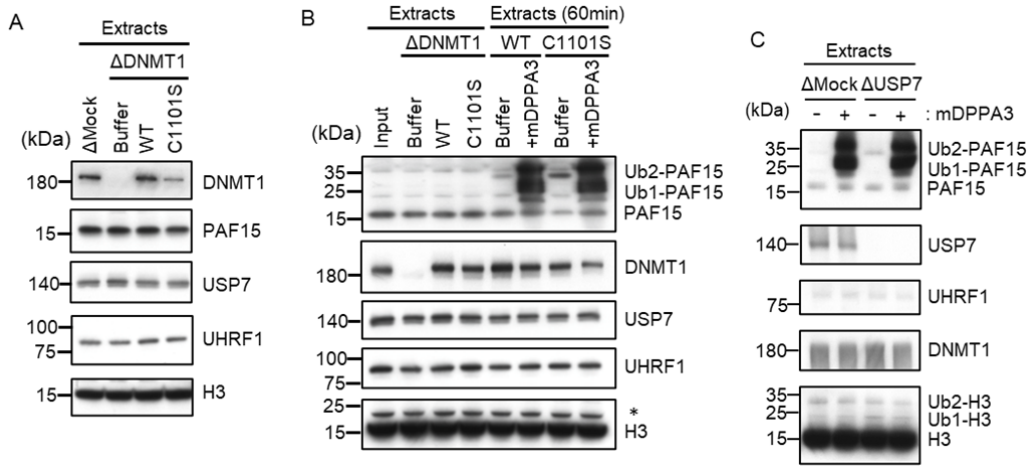

Supplemental Figure. S4 (A) rDNMT1 WT-3xFLAG or C1101S-3xFLAG were added to DNMT1-depleted extracts. The extracts used in Figure 5A were analyzed by immunoblotting using the antibodies indicated. (B) rDNMT1 WT-3xFLAG or C1101S-3xFLAG were added to DNMT1-depleted extracts used in Figure 5D. After 60 min, these extracts were supplemented with GST-mDPPA3. The extracts were analyzed by immunoblotting using the antibodies indicated. The asterisk indicates a non-specific band. (C) Replicating Mock- or USP7-depleted extracts at 90 min were supplemented with either buffer (-) or GST-mDPPA3 (+). The extracts were used in Figure 5E and analyzed by immunoblotting using the antibodies indicated. Source Data are provided as Figure S4-source data.

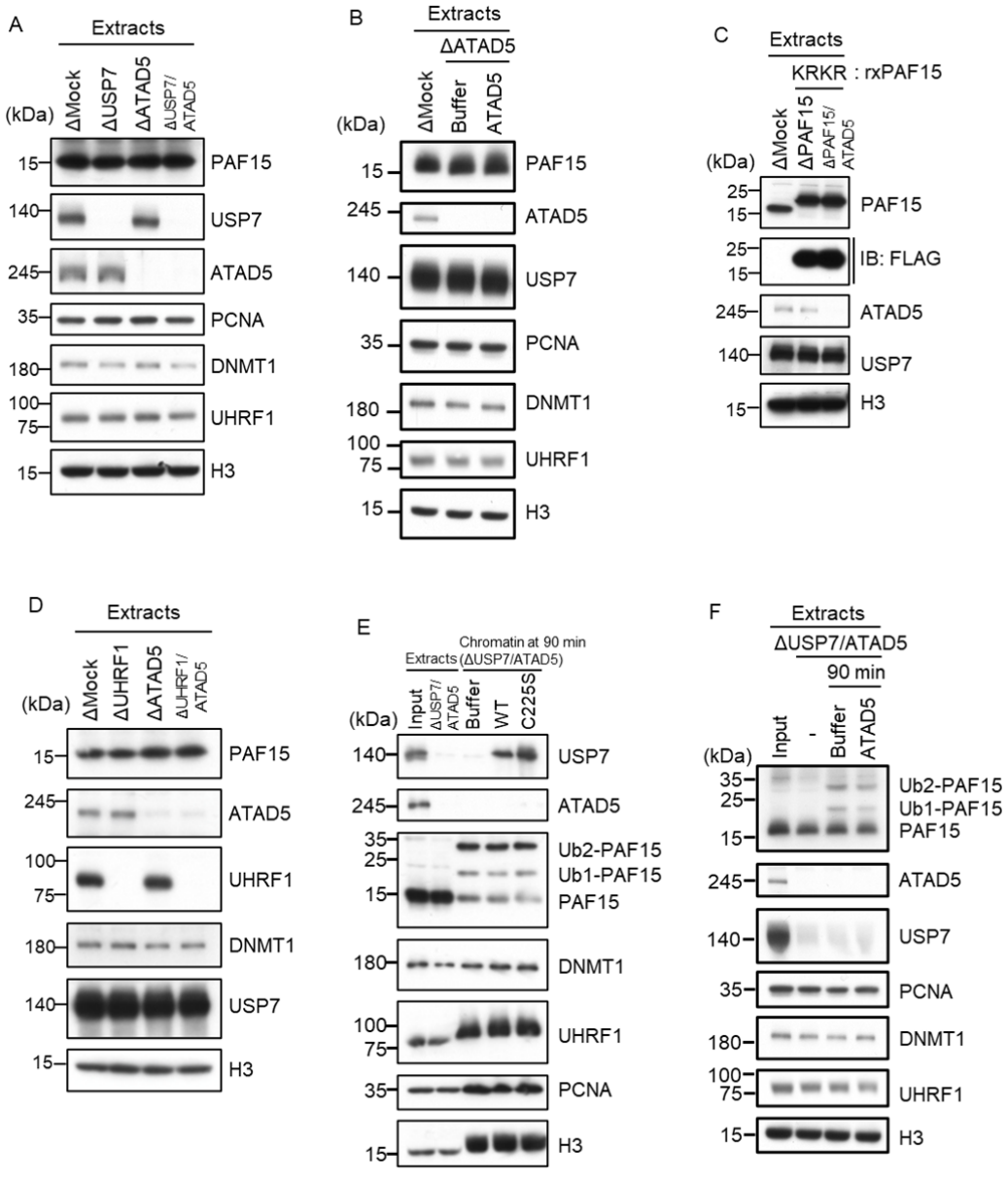

1179

Supplemental Figure. S5 (A) Mock-, USP7-, ATAD5- or USP7/ATAD5 co-depleted extracts were used in Figure 6A and analyzed by immunoblotting using the antibodies indicated. (B) rhATAD5-RFCs was added to ATAD5-depleted extracts. The extracts were used in Figure 6B and analyzed by immunoblotting using the antibodies indicated. (C) rPAF15 KRKR-3xFLAG was added to PAF15- or PAF15/ATAD5 co-depleted extracts. The extracts were used in Figure 6C and analyzed by immunoblotting using the antibodies indicated. (D) Mock-, UHRF1-, ATAD5- or UHRF1/ATAD5 co-depleted extracts were used in Figure 6D and analyzed by immunoblotting using the antibodies indicated. (E) rUSP7WT-3xFLAG or C225S-3xFLAG were added to USP7/ATAD5 co-depleted extracts. The extracts were used in Figure 6E and analyzed by immunoblotting using the antibodies indicated. (F) Replicating USP7/ATAD5 co-depleted extracts at 90 min were supplemented with either buffer or rhATAD5-RFCs. The extracts were used in Figure 6F and analyzed by immunoblotting using the antibodies indicated. Source Data are provided as Figure S5-source data.

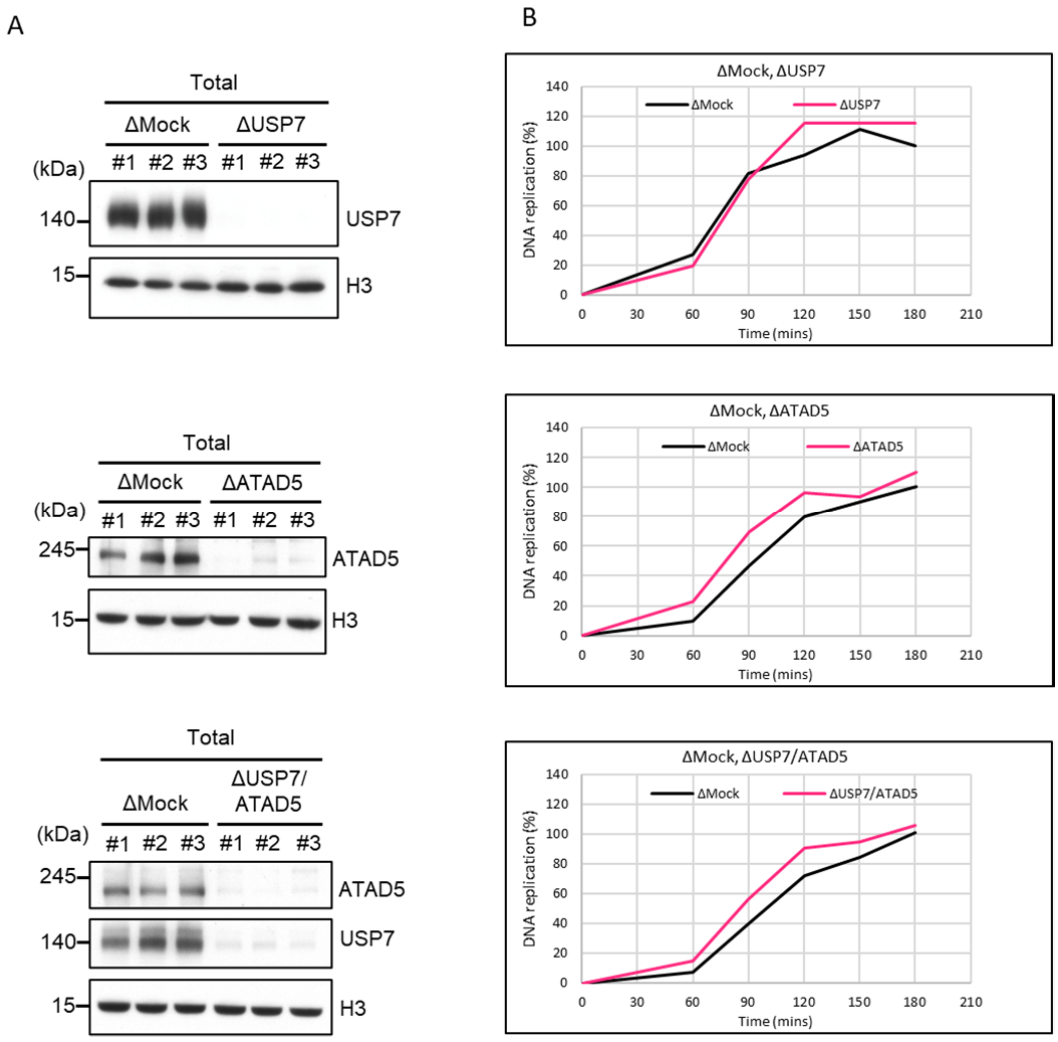

Supplemental Figure. S6 (A) Mock-, USP7-, ATAD5- or USP7/ATAD5 co-depleted extracts used in Figure 7 were analyzed by immunoblotting using the antibodies indicated. (B) Sperm chromatin and radiolabeled [α-^{32}P] dCTP were added to Mock-, USP7-, ATAD5- or USP7/ATAD5 co-depleted extracts. Purified DNA samples were analyzed to determine the efficiency of DNA replication. Source Data are provided as Figure S6-source data.